AALBORG UNIVERSITY

Department of Health Science and Technology

http://www.hst.aau.dk/

Title: Detection and Classification of Movement-Related Cortical Potentials

Theme:
Applied biomedical engineering and informatics

Project period:
Masters thesis
February 1st 2012 – June 1st 2012

Project group:
1077

Group member:

Mads Jochumsen

Supervisors:
Natalie Mrachacz-Kersting
Kim Dremstrup
Imran Khan Niazi
Dario Farina

Print run: 6
Page count: 68

ABSTRACT:

Brain-Computer Interface's (BCI) role in rehabilitation has over the past years started to attract more attention. BCIs can detect neural signals and combine the information with assistive technologies which may be used for neurofeedback in rehabilitation. Induction of Hebbian associated plasticity has been shown to be possible when pairing Movement-Related Cortical Potentials (MRCPs) with electrical stimulation, the delay between these is of crucial importance. This study served to investigate the possibility of implementing such a protocol with a BCI. MRCPs from four classes in a cue-based paradigm were extracted from multi-channel scalp EEG. Classification accuracies for each possible task pair and detection performance were obtained; this was done for different spatial filters (large Laplacian filter (LLF), optimized spatial filter and common spatial pattern filter) to evaluate their performance. The classification and detection performance were combined to obtain a measure of system performance. On average (n=12) best classification accuracy was obtained for the task pair fast vs slow movements at 60% Maximum Voluntary Contraction (MVC)' using OSF (79±9%). Best detection performance was obtained for fast movements at 60% MVC using LLF (true positive rate: 85±17%). Movements were detected approximately 0.5 s before the movement onset. The system performance, combination of detection and classification, of a 2-class system correctly detected and classified the movements 61±15% of the time. The results are promising and show that this approach can be used to implement a plasticity inducing protocol where the MRCP is paired with afferent feedback from electrical stimulation in a Hebbian associated manner.

Preface

This study was done by Mads Jochumsen as part of the masters thesis in Biomedical Engineering and Informatics at Aalborg University. The report is based on the theme *Applied biomedical engineering and informatics* and written in the period from February 1^{st} 2012 until June 1^{st} 2012. The content of this report is aimed at researchers with interest in the field of brain-computer interfacing. The picture on the front page is from [Volodin, 2010].

Reading Guide

References to literature are made using the Harvard method, in which the authors last name and the year of publishing are placed in brackets, [Last name, Year]. When an in-text reference is given, the reference can subsequently be found in the Reference List, listed in alphabetical order.

Figures and tables are numbered sequentially according to their appearance in the text and the chapter in which they are placed. For example, a figure numbered as 3.2, is the second figure in chapter 3. A description of the figure or table contents is located below the object along with a reference to the source. If no reference is given, the figure or table belongs to the authors of this report.

The first time an abbreviation is used the word will be explained. Afterwards only the abbreviation will be mentioned.

The report is divided into five parts, with chapters belonging to each part. Each chapter starts with a short introduction and a description of the content. The five parts of the report are:

- Part I - Problem Analysis
- Part II - Problem Solving
- Part III - Results
- Part IV - Synthesis
- Part V - Appendix

Contents

PART I

Problem Analysis

CHAPTER 1

Introduction

Initially the prevalence and effects of stroke are described, which serves as a motivation for the continuous research in new rehabilitation protocols. The section on stroke prevalence and effects is followed by a description of plastic changes following a stroke. Appendix A contains more detail about plasticity. Finally a new promising non-invasive stimulation protocol by [Mrachacz-Kersting et al., 2012] is briefly described. This chapter is mainly based on review articles.

1.1 Stroke

Stroke is divided into two categories; ischemic and hemorrhagic [Mackay & Mensah, 2004], both lead to acute loss of brain function in a localized area [Guyton & Hall, 2005]. It is a common global health-care problem with approximately 15 million people suffering a stroke annually; out of these, five million are permanently disabled [Mackay & Mensah, 2004]. The most commonly recognized impairment, caused by stroke, is motor impairment [Thickbroom, 2007]. Up to 80% of stroke survivors will initially have an impaired upper extremity and up to one third will have residual disability [Kimberley et al., 2004; Langhorne et al., 2009]. Motor impairment is not just limited to the upper extremities; it depends on the injury site and may affect the face and lower extremities. Due to the large number of people affected by motor disabilities, much of the rehabilitation effort is aimed at recovering normal motor function [Thickbroom, 2007].

1.2 Plasticity

It has been shown that there is a cortical reorganization following an injury to the nervous system. After a stroke in the motor cortex different changes have been observed (see appendix A). In the subacute phase after a stroke a reduction of excitability of the motor cortex has been found as well as a decrease in the representation of the affected muscles. Besides the plastic changes associated with the injury, a use-dependent cortical reorganization may occur, which may increase the representation of unaffected body parts. See Liepert et al. [2000] for a review about plastic changes following a stroke. Induction of plasticity may occur in three different ways; learning, injury, and artificially induced [Thickbroom, 2007]. It has been shown that plasticity can be induced artificially with different non-invasive stimulation protocols, with the common goal of improving motor function. It is hypothesized that induction of plasticity in the affected part of the brain is correlated to improved motor function [Cooke & Bliss, 2006; Thickbroom, 2007]. Protocols that have induced plasticity are e.g. repetitive electrical stimulation, repetitive transcranial magnetic stimulation, functional electrical stimulation (FES) and paired associative stimulation (PAS) [Everaert et al., 2009; Khaslavskaia et al., 2002; Stefan et al., 2000; Ziemann et al., 2008] (for a review on different rehabilitation techniques see [Langhorne et al., 2009; Ziemann et al., 2008]). An interesting novel approach for inducing plasticity was introduced by [Mrachacz-Kersting et al., 2012] where Movement-Related Cortical Potentials (MRCPs) are paired with afferent feedback from electrical stimulation. The afferent feedback must coincide with the MRCP so the timing of the electrical stimulation is of crucial importance. It is believed that the changes seen from this technique are Long-Term Potentiation (LTP)-like effects. LTP is a model describing synaptic plasticity, which rely on Hebbian learning rules [Hebb, 1949]. That the effects of the technique are LTP-like is based on the fulfillment of the following conditions [Mrachacz-Kersting et al., 2007][Wolters et al., 2003]:

- Rapidly evolving effect.
- Persistence even after the stimulation has stopped.
- Specific temporal order of the two stimuli.
- Reversibility.

Using the protocol by [Mrachacz-Kersting et al., 2012] the group at Aalborg University has obtained promising results in stroke subjects (not published yet), therefore this project will focus on implementing this promising idea. The pairing of MRCPs with electrical stimulation can be obtained by detecting MRCPs from the continuous electroencephalogram (EEG) with a Brain-Computer Interface (BCI) [Niazi et al., 2011, 2012] that will pair the detection of the MRCP with electrical stimulation.

CHAPTER 2

Brain-Computer Interface

This chapter is based on several review articles written by some of the major contributors to BCI research. Initially a BCI system is defined. In the following section a schematic representation of a BCI is described and finally some of the applications of a BCI are outlined with emphasis on BCI's role in rehabilitation.

2.1 BCI Definition

Several definitions of a BCI exist, two of the most well-known are:

- "*A BCI is a communication system in which messages or commands that an individual sends to the external world do not pass through the brain's normal output pathways of peripheral nerves and muscles.*" [Wolpaw et al., 2002]
- "*BCI describes any computerized system, which involves information obtained from the brain. The BCI system interprets specific brain activity without using the brain's normal output pathways of peripheral nerves and muscles to work directly with external devices or applications*".[Birbaumer & Cohen, 2007]

Furthermore BCIs can be divided into two different modes; asynchronous or synchronous. The asynchronous BCI (self-paced) is always active and besides reacting to the predetermined mental tasks that control the system, it is also able to identify a rest state or idle state. On the contrary the synchronous (cue-based) BCI depends on a specific protocol [Wolpaw et al., 2002].

2.2 Schematic Presentation of a BCI System

A BCI system normally consists of the following parts:

- Signal acquisition
- Preprocessing
- Feature extraction
- Classification

Brain signals are recorded after which they are being preprocessed to enhance the signal-to-noise ratio (SNR). When the SNR has been improved the feature extraction takes place. These features are sent to a translation algorithm/classifier that decodes the user's intent and translates it into device commands (see figure 2.1).

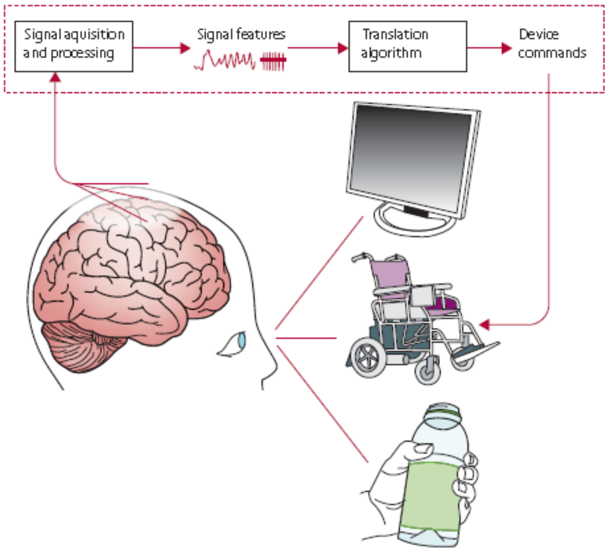

Figure 2.1: *The BCI system records signals from the brain. The signals are processed and certain features are extracted. A translation algorithm transforms the features into device commands. Page 1033 in [Daly & Wolpaw, 2008].*

Signal Acquisition

In BCI research three different recording locations have been used; scalp EEG, electrocorticography (ECoG) from the cortical surface, and neuronal action potentials and local field potentials from the cortex. Each technique has advantages and disadvantages. EEG is easy and safe to record, but it has limited resolution and a limited frequency range. ECoG has higher resolution, but long-term stability and biocompatibility are unknown plus the procedure is invasive. Signals acquired from the cortex has the highest resolution, but the same problems apply as for ECoG. Other techniques can be used for BCI such as; magnetoencephalography, functional Magnetic Resonance Imaging, Positron Emission Tomography and functional near-infrared imaging.[Daly & Wolpaw, 2008]

The acquired signals that can be used for BCI control can be summarized in the following table:

- Visual evoked potentials.
- Slow cortical potentials.
- P300 potentials.

- Mu or beta rhythms (sensorimotor rhythms).
- Electrical neuronal activity recorded from the cortex and cortical surface.

In [Wolpaw et al., 2002] the different control signals and their application in some present-day BCIs are explained and discussed in detail.

2.2.1 Preprocessing

Preprocessing of the control signal is essential due to a very low SNR, especially the control signal of interest in this study; MRCP. Control signals derived from the EEG are contaminated with various artifacts of technical and physiological origin [Sörnmo & Laguna, 2005]. The most common artifacts are 50 Hz noise, muscle activity and Electrooculography (EOG). EOG is a problem when working with MRCPs due to an overlapping frequency range (MRCP: 0–5 Hz, EOG: 0–38 Hz). EOG has a high amplitude (around 100 μV peak-to-peak) compared to MRCPs (around 15–20 μV peak-to-peak, see figure 5.4).

To improve the poor SNR of the control signals different approaches to remove noise have been proposed; this includes different filters such as highpass, lowpass and bandpass, which may be applied to remove e.g. muscle activity and 50 Hz noise. Different types of spatial filters have also been applied to correct for the blurring that may arise from lowpass filtering. E.g. Laplacian filter reduces common activities between neighboring electrodes and improves spatial resolution; it reduces distant sources and local sources are increased. In [Niazi et al., 2011; Wolpaw et al., 2002] different spatial filters are compared.

2.2.2 Feature Extraction

After the preprocessing of the signals, time or frequency domain features may be extracted. Examples of time domain features are amplitudes of slow cortical potentials (see section 5.4 for examples of MRCP features) or neuronal firing rates. Features from the frequency domain can be amplitudes from sensorimotor rhythms. It is possible to combine features from the time and frequency domain and thereby improve performance [Schalk et al., 2000] (see [Wolpaw et al., 2002] for a review).

2.2.3 Classification

When signal features have been extracted from the control signal the classifier translates the signal features into device commands reflecting the user's intent (see [Lotte et al., 2007] for a review on different classification techniques applied for BCI purposes). Different methods for classification have been proposed such as linear and nonlinear methods. A good classifier should adapt to the user at three different levels [Wolpaw et al., 2002]:

- Classifier must adapt to the specific user (e.g. amplitude of event-related potential).
- Online adjustments to reduce the effect of spontaneous variations (e.g. fatigue).
- Mutual learning: The classifier trains the user and vice versa (e.g. if the feature is an amplitude of an event-related potential, the correlation between amplitude and user intent should increase over time).

2.3 Applications

Since the beginning of BCI research two major fields have been investigated; communication and control. Applications for word processing, communication aid for amyotrophic lateral sclerosis (ALS) patients, controlling wheel chairs, and other types of environmental control have been developed (see [R. Millán et al., 2010] for a recent review of BCI control of assistive technologies). These aids are helping to improve the quality of life for patients suffering from severe neuromuscular disorders, such as ALS, stroke, and spinal cord injury [Wolpaw et al., 2002]. Besides BCI use in communication and control, neurological rehabilitation has started to attract attention [Daly & Wolpaw, 2008][Meng et al., 2008][Daly et al., 2009].

Rehabilitation

In functional recovery it is important to target the impairment as directly as possible through activity-dependent plasticity [Nudo, 2006; Wolpaw & Tennissen, 2001; Ziemann et al., 2004]. The expectation of current therapies is that repetitive movement practice will induce plasticity in the central nervous system (CNS) and thereby improve motor function. A BCI approach is to use the brain activity to guide plasticity and thereby improve motor function, and also motivate and involve the patient [Daly & Wolpaw, 2008].

In figure 2.2 two training strategies (A and B) are proposed that will lead to the goal, which is restored CNS function. Strategy A is based on the hypothesis that training the brain activity to become normal will lead to better CNS functioning, which will then lead to improvements in motor control, it has been supported by several studies e.g. [Decety, 1996; Stinear et al., 2006; Weiss et al., 1994]. Strategy B is based on detection of brain activity (e.g. MRCP) that will trigger an external device, which will assist the movement (e.g. FES [Daly et al., 2009] or robot-assistance [Gomez-Rodriguez et al., 2010]). The sensory feedback provided from the movement is thought to induce CNS plasticity and improve the motor function [Daly & Wolpaw, 2008]. The fundamental idea behind this strategy was discussed at the 4$^{\text{th}}$ International BCI Meeting 2010 in Asilomar, CA, USA [Grosse-Wentrup et al., 2011].

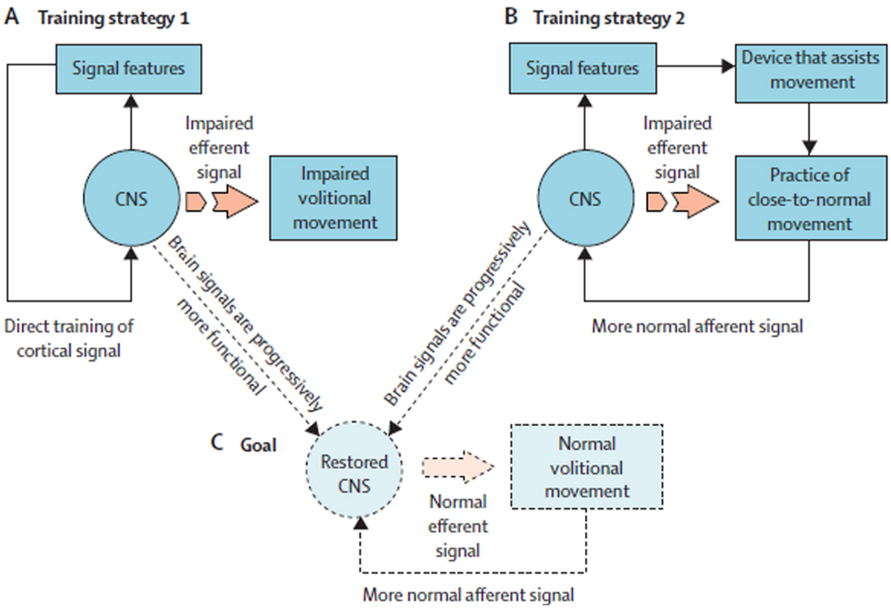

Figure 2.2: *Two training strategies are proposed for induction of CNS plasticity restoration of motor function. Strategy A relies on training of brain activity to become closer to normal, while strategy B will trigger a device that assists movement and thereby provide feedback. Page 1039 in [Daly & Wolpaw, 2008].*

CHAPTER 3

Movement-Related Cortical Potentials

This chapter gives an introduction to the type of MRCP seen for externally cued movements. MRCPs for self-paced or internally driven movements are known as Bereitschaftspotentials (BPs) [Shibasaki & Hallett, 2006], and MRCPs for externally cued movements are known as Contingent Negative Variation (CNV) [Walter et al., 1964]. BP and CNV are not only seen in tasks involving real movements, but also in imagined motor tasks [Jankelowitz & Colebatch, 2002; Nascimento et al., 2006]. The protocol in this study used cue-based movements with variations of speed and torque amplitude, therefore the effect of movement parameters on MRCPs in general is outlined.

3.1 Contingent Negative Variation

In 1964 [Walter et al., 1964] described the movement-preceding negativity of signaled (cued) movements; this is known as CNV. The CNV is an index for expectancy and a sign of sensori-motor association that reflects processes involved in preparation of voluntary movements [Walter et al., 1964]. CNV can be elicited in a simple paradigm such as a forewarned reaction time task [Brunia, 2003]. In this paradigm, a warning signal/stimulus (S1) informs the subject of an upcoming second stimulus (S2) after which the subject has to react/respond [Brunia, 2003].

Morphology of the CNV

The negativity between the two stimuli has been divided into two phases when recorded with a relatively long interstimulus interval; early CNV and late CNV (see figure 3.1) reflecting different neuronal generators [Connor & Lang, 1969; J. W. Rohrbaugh et al., 1976]. The amplitude of the early CNV tends to decrease from a larger early CNV (after the warning stimulus, S1) to a smaller late CNV (approaching the response stimulus, S2) over the anterior parts of the scalp. The opposite is the case over the posterior parts of the scalp; an increase is seen from a smaller early CNV to a larger late CNV [Cui et al., 2000]. The early CNV persists for approximately 1-1.5 s after the warning stimulus while the late CNV starts to develop approximately 1 s before the response stimulus [Hamano et al., 1997].

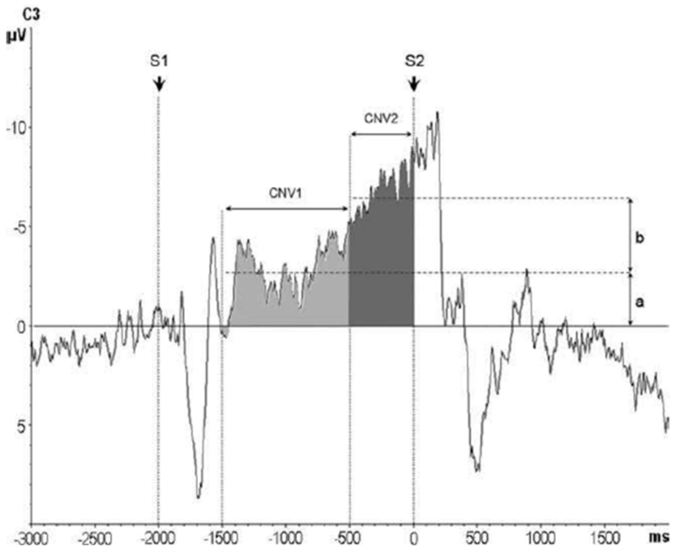

Figure 3.1: *CNV is seen between the two stimuli; S1 and S2. The CNV is divided into an early phase (CNV1) and a late phase (CNV2). The figure is from page 6 in [Lu et al., 2011].*

Generators of the CNV

A lot of attention and effort have been devoted to find the neural generators of the CNV, however, the generators and their contribution to the CNV are not entirely known since the CNV is a summation of multiple cortical potentials with different functions and origins (see [Brunia, 2003] for a review). The late CNV has been hypothesized in several studies to be similar to the BP (e.g. [Hultin et al., 1996]), but this hypothesis has been rejected by several studies (e.g. [Cui et al., 2000; Hamano et al., 1997; Lu et al., 2011]). The early CNV is distributed over the prefrontal area and supplementary sensorimotor area (SSMA), while the late CNV is distributed over the prefrontal area, primary motor and sensory cortex, temporal area, occipital area and SSMA [Deiber et al., 1996; Hamano et al., 1997; Ikeda et al., 1996]. The role of the prefrontal cortex as a generator has been outlined in several animal studies where CNV was recorded from the prefrontal area as well as premotor and primary motor area [Borda, 1970; Donchin et al., 1971; McSherry & Borda, 1973]. A positron emission tomography (PET) study done by [Deiber et al., 1996] also found contribution to the generation of CNV from the cerebellum, basal ganglia, and the thalamus. [Ikeda et al., 1997] reported that especially the basal ganglia among the subcortical structures contribute to the late CNV, while [Ikeda et al., 1994] suggested that the cerebellum did not contribute to the CNV. The role of the premotor cortex in the generation of the CNV has been described in a number of studies [Deiber et al., 1996; Grafton et al., 1998; Lu et al., 2011]. It is hypothesized that the premotor cortex is responsible for detecting cues [Deiber et al., 1996; Matsumoto et al., 2003], and is active in motor preparation [Kurata & Hoffman, 1994; Matsumoto et al., 2003; Simon et al., 2002]. [Matsumoto et al., 2003] discuss the role of different subdivisions of the premotor cortex. The cognitive function is represented in the rostral premotor cortex and motor functions in the caudal premotor cortex leading to a cognitive-motor gradient (rostrocaudal) in the premotor cortex during a CNV task [Crammond & Kalaska, 2000; Matsumoto et al., 2003]. The dorsal premotor cortex (PMd) is believed to play an important role in coupling arbitrary sensory cues to motor acts and response selection [Chouinard et al., 2003; Crammond & Kalaska, 2000]. The response in PMd is maximally evoked by the apperance of the warning stimulus in the CNV paradigm [Crammond & Kalaska, 2000]. Recently in a study by [Lu et al., 2011] it was proved (by using rTMS) that the PMd is more involved in preparatory processes of externally cued movements compared to self-initiated movements, an opposite role was found for the SMA. This study supports the findings from earlier animal studies [Kurata & Wise, 1988; Mushiake et al., 1991].

Electrode Placement

As mentioned, the amplitude of the early CNV tends to decrease from a larger early CNV to a smaller late CNV over the anterior parts of the scalp, while the opposite is the case over the posterior parts of the scalp [Cui et al., 2000]. [Cui et al., 2000] found that the largest negative potential occurred mainly at frontal (F) frontocentral (FC) and central (C) regions for the early CNV, while the late CNV moved from the anterior to the middle part of the scalp and displayed the largest potentials at FC, C and centroparietal (CP) regions. [Yazawa et al., 1997] reported that the largest amplitude of the late CNV was found over Cz in a dorsiflexion task, the same was the case for wrist flexions [Ikeda et al., 1997].

Interpretation of the CNV

According to [Ikeda et al., 1997] the CNV represents neuronal activity necessary for sensorimotor integration or association related to planning or execution of cued movements. The early CNV largely reflects sensory information of the warning stimulus, while the late CNV represents motor readiness and preparatory activity of a forthcoming motor response [Hamano et al., 1997; J. W. Rohrbaugh et al., 1976]. If the time interval between the warning and response stimulus is short then it is difficult to disentangle processes related to anticipatory and movement preparation [Brunia, 2003]. If the time interval is long then the stimulus-related contamination resolves and a cleaner (in the sense of pure motor) late CNV is seen [Cui et al., 2000]. In the CNV paradigm the following terms have been associated: Cognition, attention, judgment, expectation, estimation, determination, planning, preparation and motor processing [Cui et al., 2000; Ikeda et al., 1996; Walter et al., 1964; Yazawa et al., 1997].

Factors Affecting the CNV

As indicated in the previous paragraph several factors affect the CNV such as attention and motivation [Brunia, 2003]. Especially attention has been reported as an important factor [Cui et al., 2000; Ikeda et al., 1996; Yazawa et al., 1997]. [Wise et al., 1997] also reported that proprioceptive, visual, gaze and attentional information help in producing an output that reflects selection, preparation and execution of movements. [Tecce, 1972] demonstrated that peripheral arousal (such as increased heart rate) modulates the CNV amplitude (particularly the early CNV). This was also demonstrated in a study by [Nagai et al., 2004], where it was argued that the CNV is an index of cortical arousal during orienting and attention. Another factor affecting the CNV is the complexity of a movement, [Cui et al., 2000] found larger CNV amplitudes prior to complex movements than prior to simple movements. Increased muscular effort results in increased amplitude for the late CNV [J. Rohrbaugh & Gaillard, 1983]. An increase in the CNV amplitude was also observed when comparing fast responses with slow responses [Brunia & Vingerhoets, 1980]. In task execution an increase in negativity parallel to an increased memory has been reported [Ruchkin et al., 1992]. Uncertainty of timing is a factor that has been reported to reduce the amplitude of the CNV [Brunia, 2003]. [Brunia, 2003] reviews the findings of several studies regarding the amplitude of the CNV based on the information provided to the subject prior a response. All in all the studies can be divided into two categories; the first category is an increase in CNV amplitude when there is uncertainty about a response (such as speed required for a contraction), while the second category is an increase in CNV amplitude when there is no uncertainty about a response. [Brunia, 2003] discusses that the amplitude of the CNV may increase in the sensory domain with increasing uncertainty, while an increase in amplitude may be observed in the motor domain when no uncertainty of the task exists. Lastly [Ikeda et al., 1997] found that the amplitude of the late CNV was reduced in patients suffering from Parkinson's disease.

3.2 Movement Parameters Effect on MRCPs

Motor tasks are characterized by a number of movement-related parameters such as speed/rate of torque development (RTD), force/-

torque amplitude, and movement direction. Torque amplitude and RTD have been shown, in several studies, to be reflected in the preparation and execution of different motor tasks (see figure 3.2).
The effect of torque amplitude alone on the MRCP has provided different results. [Ray et al., 2000] found that increased torque amplitude increased the amplitude of the MRCP, [S. M. Slobounov & Ray, 1998] found an increase in the movement-monitoring potential and [Nascimento et al., 2005] in the readiness potential. [Gu, Nascimento, et al., 2009; Nascimento et al., 2006; Romero et al., 2000] reported that different torque amplitudes could be differentiated in motor imagery as well. On the other hand [S. Slobounov et al., 2004, 2002, 2000] reported that different torque amplitudes could not be differentiated in the MRCP.
RTD, however, are generally accepted to modulate the MRCP in motor tasks and motor imagery tasks. The amplitude of the BP, CNV and movement-monitoring potential has consistently been reported to increase with increasing RTD of the movement (or imagined movement) [Brunia & Vingerhoets, 1980; Cooper et al., 1989; Grünewald & Grünewald-Zuberbier, 1983; Nascimento et al., 2005, 2006; Ray et al., 2000; S. M. Slobounov & Ray, 1998]. Differentiation between different levels of RTD has been accomplished [Farina et al., 2007; Gu, Dremstrup, & Farina, 2009; Gu, Nascimento, et al., 2009; Nascimento & Farina, 2008].

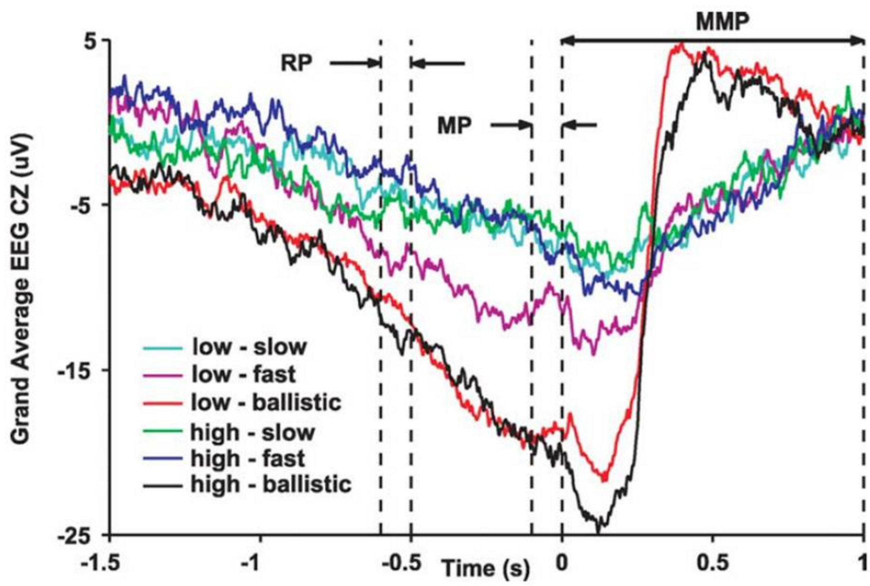

Figure 3.2: *Each graph represents an isometric plantar flexion task (torque amplitude/RTD) from nine subjects. Six different movements were executed for the combination of two different torque amplitudes and three different RTDs. Time 0 is the onset of the movement. The figure is from page 159 in [Nascimento et al., 2005].*

Most of the studies dealing with the effect of movement parameters on MRCPs are based on isometric contractions. [Fang et al., 2004] compared eccentric and concentric movements and found larger amplitudes of the MRCPs in eccentric movements (mainly in the late BP), and [Gu, Dremstrup, & Farina, 2009] compared imagination of two dynamic movements which could not be discriminated.

CHAPTER 4

Aim

The Problem Analysis is briefly summarized with emphasis on BCI-driven electrical stimulation for rehabilitation purposes. This serves as motivation for doing this project. In the end of this chapter the aim of this project is stated.

Stroke is a devastating disease, affecting many people, which can lead to motor disabilities [Mackay & Mensah, 2004]. A lot of research is conducted to help disabled stroke victims regain some of the lost functionality of a limb [Thickbroom, 2007].
After the injury of a stroke, plastic changes occur and a use-dependent cortical reorganization may occur, which may increase the representation of unaffected body parts [Liepert et al., 2000]. Reversing these plastic changes may be mediated through induction of Hebbian associated plasticity in the representations of the affected body parts and a use-dependent cortical reorganization may occur, which is hypothesized to improve motor function [Cooke & Bliss, 2006] (see chapter 1 and appendix A).
One method for inducing Hebbian associated plasticity in the CNS was proposed by [Mrachacz-Kersting et al., 2012]. They modified the PAS protocol [Stefan et al., 2000] so a physiological signal, MRCP, was paired with peripheral electrical stimulation, the result of using this protocol was an increase in corticospinal excitability, functional improvement in stroke subjects has also been observed (not published yet).
A way to implement this protocol could be accomplished with a BCI, which role in rehabilitation has started to attract attention in the BCI community over the past years (see [Daly & Wolpaw, 2008; Grosse-Wentrup et al., 2011] and section 2.3).
Instead of using peripheral electrical stimulation a BCI could be implemented to control FES so a movement intention can be paired with a movement produced by the FES and that the sensory feedback coincide with the motor potential of the MRCP (MP) to produce Hebbian associated plastic changes [Mrachacz-Kersting et al., 2012]. A recent study by [Daly et al., 2009] outlined the possibility of using a BCI as a controller for FES.
To control FES, however, requires different control parameters such as velocity and applied forces [Popovic & Sinkjær, 2000]. These con-

trol parameters have been shown to affect the MRCP in motor and motor imagery tasks, mainly involving isometric contractions (see section 3.2). The ultimate goal would be to detect and decode the early phase of an MRCP to determine the RTD and torque amplitude of a forthcoming movement online; this would lead to more sophisticated and natural control of FES compared to a binary selection (on/off).
[Farina et al., 2007; Gu, Nascimento, et al., 2009; Nascimento & Farina, 2008] have investigated if RTD and force amplitude can be classified from single-trial EEG traces of different isometric movements and motor imagery tasks; they showed it was possible to classify the different movements and motor imagery tasks relatively successfully. Before the classification of MRCPs can take place they have to be detected from continuous recordings. Niazi et al. [2011] successfully detected MRCPs in continuous EEG recordings when simulating an online BCI system, and in a real online system using self-paced movements [Niazi et al., 2012].

This study had three purposes:

- To evaluate the classification of single-trial MRCPs for cue-based isometric contractions of the tibialis anterior muscle, with different levels of torque amplitude and RTD, based on features extracted from the initial negative phase of the MRCP. Furthermore, the classification accuracy was evaluated for features extracted from the complete MRCP (initial negative phase + reafferent potential) as a comparison.
- To detect single-trial MRCPs in a simulated real-time BCI.
- To evaluate the performance of a BCI system by combining detection with classification.

PART II

Problem Solving

CHAPTER 5

Methods

Initially the experimental protocol will be explained, which includes the different tasks the subjects performed as well as the different recordings. The following section describes the data pre-processing with emphasis on different spatial filtering techniques used in the classification and detection of MRCPs. The features are briefly described as well as the classification, which was performed with a support vector machine (SVM). Lastly the detection and system performance are explained.

5.1 Experimental Protocol

12 healthy volunteers aged 22–42 (4 women and 8 men; mean age: 27±6 years) participated in this study. The subjects were asked to perform four different tasks of real isometric dorsi-flexions. The tasks were all possible combinations of two different torque amplitudes and two different RTD. The torque amplitude was either 20% MVC or 60% MVC and RTD was set to either 0.5 s or 3 s to reach the desired torque amplitude. The subjects were instructed during the preparation of the recording sites of the scalp. The subjects spent approximately 5 minutes familiarizing with each task, they were all naive to the tasks. The tasks were to produce torque (force transducers mounted on a pedal where the foot was fixated) and match it to four different templates (see figure 5.1), a custom made program was used for this purpose where torque was used as input (*Follow Me* by Knud Larsen, SMI, Aalborg University).

The subjects were seated in an ergonomic chair two meters from the screen, which displayed *Follow Me*, in an electrically shielded room.
The four tasks were randomized in blocks consisting of 50 trials.
The subjects were asked to focus their gaze at the center of the screen to avoid slow eye movements and to avoid eye blinks and facial muscle movements during the tasks.

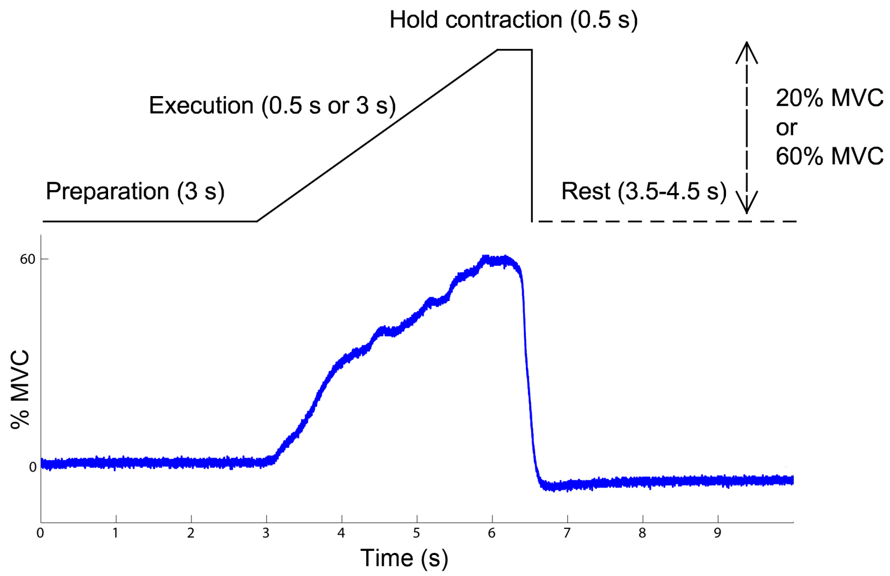

Figure 5.1: *The top figure is a schematic representation of the template the subjects had to match. The bottom figure is the torque produced during 60% MVC with a RTD at 3 s.*

5.2 Signal Recordings

EEG

The EEG and EOG recordings were amplified by a NuAmp (DC-coupled 22 bit AD monopolar amplifier, from Neuroscan Labs, Neurosoft. Inc) and aquired with Neuroscan 4.5 (Acquire module) at 500 Hz. Self-adhesive disposable electrodes ($Ambu^R$ Blue Sensor M. Ref: M-00-A/50.) were mounted at the following position according to the International 10-20 System [Klem et al., 1999]: F3, Fz, F4, C3, Cz, C4, P3, Pz and P4. The EEG recordings were referenced and grounded to similar self-adhesive disposable electrodes on the right earlobe (A2) and at nasion respectively. EOG was recorded above the left eye. Electrode impedances were kept below 5 kΩ for all subjects.

Torque

The ankle dorsi-flexion torque was measured on a pedal instrumented with force transducers. The torque signal was input to an A/D board (National Instruments) and used for cursor control in '*Follow Me*'. The torque signal was also acquired with '*Mr. Kick*' (Knud Larsen, SMI, Aalborg University) at a sampling frequency of 2 kHz. In the beginning of the experiment the MVC was recorded. MVC was defined as the highest torque produced out of three recordings each separated by 30 to 60 s.
The movement onset was used to synchronize the trials (in figure 5.1 the movement onset is at 3 s), so a movement starting to early or late would not confound the results.

5.3 Data Pre-processing

In figure 5.2 an overview of the data import from Neuroscan to Matlab is shown, this was done with EEGLAB. The force was imported using a custom-made Matlab script. After the data was imported,

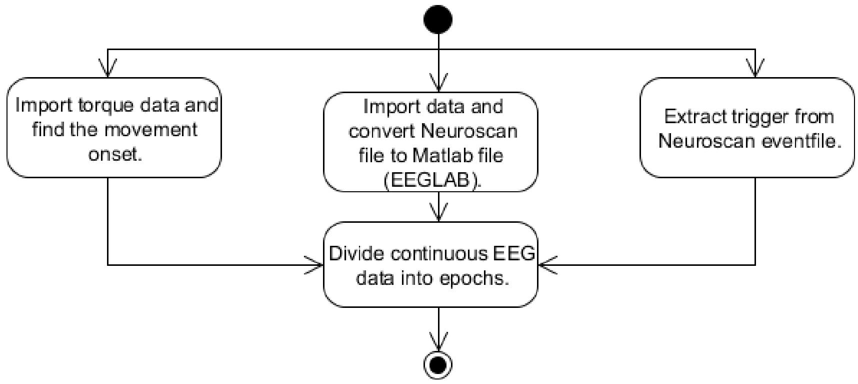

Figure 5.2: *An overview of the data import steps. The different steps are described in more detail in the corresponding sections.*

synchronized and divided into epochs it was filtered with a 2^{nd} order Butterworth zero-phase digital band-pass filter from 0.05 Hz to 5 Hz followed by a similar Notch filter from 49 Hz to 51 Hz. The discrete wavelet transform (DWT) was also tested as a pre-processing method, but it was not used for further analysis (see appendix B for a description of the DWT).

Spatial Filtering

Spatial filtering is a useful technique in single-trial EEG analysis in order to improve the poor SNR. Due to volume conduction the multichannel EEG recordings give a signal which is a blurred image of the brain activity; spatial filters can correct for this blurring [Blankertz, Tomioka, et al., 2008]. In this study four different spatial filters were evaluated (see figure 5.3).

Large Laplacian Filter

The Large Laplacian filter (LLF) is a filter with fixed coefficients based on sensor geometry. The filter improves the spatial resolution of scalp potentials by reducing the common activities between neighboring electrodes. The filter reduces the effect of distant sources and enhances local sources [Dastmalchi, 2003].

$$\text{Laplacian} = V_0 - \frac{1}{8} \cdot (V_1 + V_2 + V_3 + V_4 + V_5 + V_6 + V_7 + V_8) \qquad (5.1)$$

V_0 is the voltage at the center electrode (Cz) and V_{1-8} are the voltages at the surrounding electrodes. The coefficients must sum up to zero so the filter has high pass characteristics (see [Dastmalchi, 2003] for more detail about Laplacian filtering).

Common Spatial Pattern

Common Spatial Pattern (CSP) filter is a spatial filter which can be optimized for each subject in a data dependent fashion similar to the optimized spatial filter and unlike the fixed Laplacian filter i.e. it is a subject specific spatial filter. The purpose of the CSP filters is to maximize the variance of the spatially filtered data in one condition and minimize the variance for the other. A way to implement the CSP algorithm is [Blankertz, Tomioka, et al., 2008]:

$$S_d = \sum^{(+)} - \sum^{(-)} S_c = \sum^{(+)} + \sum^{(-)} \tag{5.2}$$

S_d corresponds to the discriminative activity found by the difference between the estimate of the covariance matrices ($\sum$) for the two conditions ('+' and '-'), in this study the two conditions were 'signal' and 'noise'. S_c corresponds to the common activity in the two conditions, which is not desired. The spatial filter coefficients which maximizes the variance in one condition and minimizes it in the other can be found by solving the following maximization problem:

$$maximize_{w \in R^c} \frac{w^T S_d w}{w^T S_c w} \tag{5.3}$$

It is important that the eigenvalue for the filter (w) in equation 5.3 is high, which will lead to high variance in condition 1 and low variance in condition 2. If a low eigenvalue is used there will be low variance in condition 1 and high variance in condition 2. For more detail about CSP see [Blankertz, Tomioka, et al., 2008; Kawanabe et al., 2009].

Optimized Spatial Filter

The purpose of the Optimized Spatial Filter (OSF) was to find a linear combination of the recorded EEG channels that would maximize the MRCP energy while minimizing the noise energy. The filter coefficients were optimized based on a training set consisting of 'signal' and 'noise' epochs (equation 5.4 and 5.5) of 3 s duration (signal: -2 to 1 s around peak negativity, noise: -6 to -3 s with respect to peak negativity). The signal and noise epochs were rejected if they contained observable EOG artifacts.

$$S_i(t) = \sum_{k=1}^{N_{ch}} x_k \cdot S_{i,k}(t) \tag{5.4}$$

$S_i(t)$ is the i^{th} signal epoch and $N_i(t)$ is the i^{th} noise epoch.

$$N_i(t) = \sum_{k=1}^{N_{ch}} x_k \cdot N_{i,k}(t) \tag{5.5}$$

N_{ch} is the number of EEG channels (in this case 9), x is the vector containing the filter coefficients:

$$x = (x_1, ..., x_c) \tag{5.6}$$

Based on the signal and noise epochs the SNR was calculated (equation 5.7).

$$\mathrm{SNR} = 10 \cdot log_{10}(\frac{P_S}{P_N}) \tag{5.7}$$

where P_S and P_N are the power of the signal and noise epochs.

The purpose of the optimization was to find the set of filter coefficients (x) that produced the highest SNR in the training set, the filter coefficients had to sum up to zero so the spatial filter had high-pass characteristics [Dastmalchi, 2003]. The optimization was performed with a quasi-Newton method. Three steps were repeated until x converged to the solution (maximum SNR). The initial guess of x was the coefficients of the EEG Large Laplacian montage and an approximated Hessian matrix. The three steps that were repeated are:

- Step 1: Find the direction of the next step.
- Step 2: Line search (finding a local minimum) to find an acceptable step size.
- Step 3: Update the Hessian matrix (Broyden–Fletcher–Goldfarb–Shanno method [Byrd & Nocedal, 1989]).

This section was based on the work of [Niazi et al., 2011], more detail about the computation of the OSF are provided in that article. [Niazi et al., 2011] found that the OSF outperformed the LLF and CSP filter.

5.4 Feature Extraction

As mentioned in section 3.2 RTD has been shown, in several studies, to modulate the amplitude of the early CNV, late CNV, BP and movement-monitoring potential. The effect of torque level on the MRCP, however, has shown different results, but an increased torque amplitude has lead to; an increase in MRCP amplitude, an increase in the movement-monitoring potential and readiness potential.
These observations are present when averaging several trials, but classification of RTD and torque amplitude based on single trials has been accomplished. In the table below the features that have been used in the classification of RTD and torque amplitude in single trials are listed.

- [Farina et al., 2007]: classification of RTD and torque amplitude using DWT marginals.

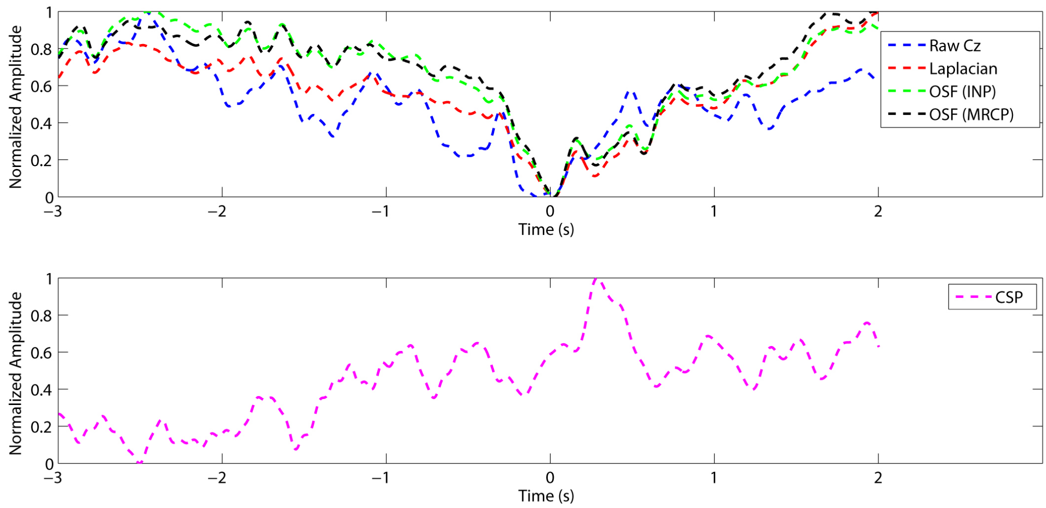

Figure 5.3: *In the top figure a single-trial MRCP is shown when filtered with LLF, Optimized Spatial Filter (OSF) based on the Initial Negative Phase (INP) and OSF based on the complete MRCP. The bottom figure shows the output of the filter found from the Common Spatial Pattern (CSP) algorithm. Time 0 is defined as the movement onset.*

- [Nascimento & Farina, 2008]: classification of RTD using DWT marginals.
- [Gu, Nascimento, et al., 2009]: classification of RTD and torque amplitude using DWT marginals
- [Gu, Dremstrup, & Farina, 2009]: classification of RTD using the rebound rate and power of the Mu-rhythm and Beta-rhythm.
- [Gu, Farina, et al., 2009]: classification of RTD using DWT marginals.

In [Gu, Dremstrup, & Farina, 2009] the amplitude of peak negativity and the gradient of NS1 and NS2 of the MRCP were proposed as features, but no significant difference between the two RTD was obtained using these features.

In this study the features were selected based on the knowledge of MRCP averages for each task (see figure 5.4). Different features, extracted from the initial negative phase (INP) (from the start until 100 ms before peak negativity), were used for classification of RTD and torque levels. RTD and torque levels were also classified based on features that were extracted from the whole MRCP. All features were extracted from the time domain. The DWT marginals were also used in pilot tests, but they were not included due to poor classification accuracies (see appendix B for a description of the DWT marginals).

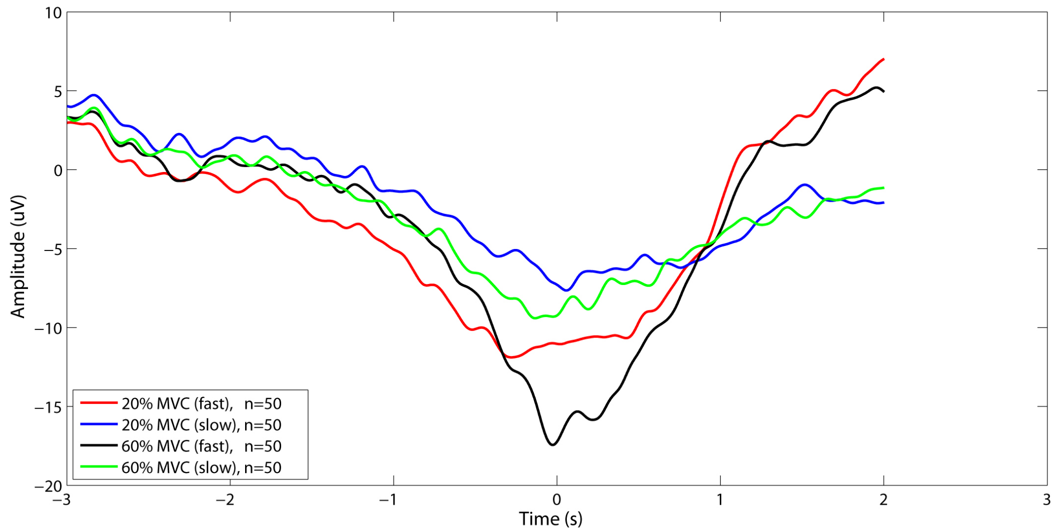

Figure 5.4: *Average of 50 trials for each task. Time 0 is defined as the movement onset.*

Feature Extraction - INP

- Intersection and slope of a linear regression based on the data from -2 s to -0.1 s before the movement onset.
- Intersection and slope of a linear regression based on the data from -0.5 s to -0.1 s before the movement onset.
- Maximum negative amplitude in the interval -2 to -0.1 s before the movement onset.
- Mean amplitude in the interval -2 to -0.1 s before the movement onset.

See figure 5.5 for an overview of the features.

Feature Extraction - INP + Reafferent Potential

The following features were extracted with the features described above:

- Intersection and slope of a linear regression based on the data from 0 s to 1 s after the movement onset.
- Maximum negative amplitude in the interval ±0.5 s around the movement onset.
- Mean amplitude in the interval ±0.5 s around the movement onset.
- Mean amplitude in the interval 0 to 0.75 s after the movement onset.

See figure 5.6 for an overview of the features.

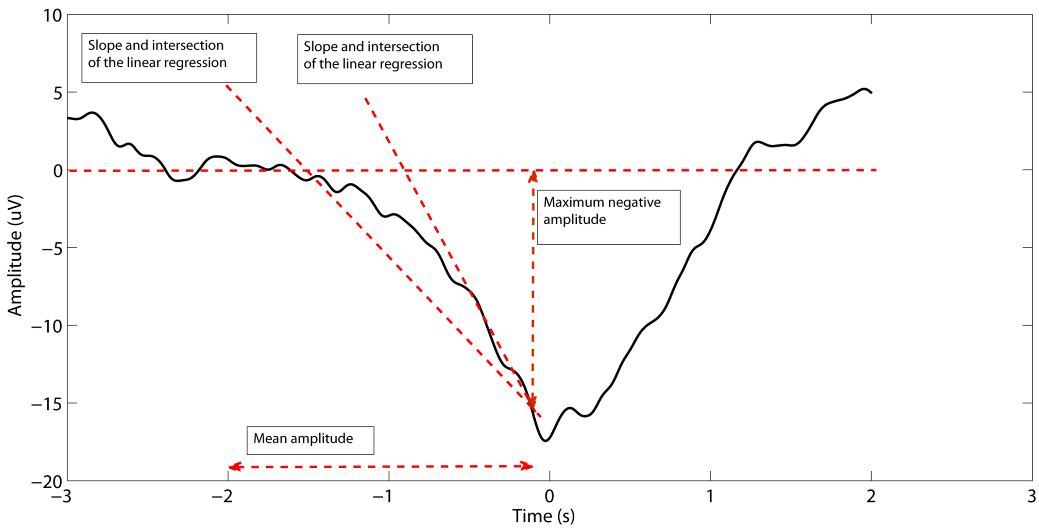

Figure 5.5: *The features were extracted from the initial negative phase from -2 to -0.1 s before the movement onset. The features are written in the black boxes. Time 0 is the movement onset.*

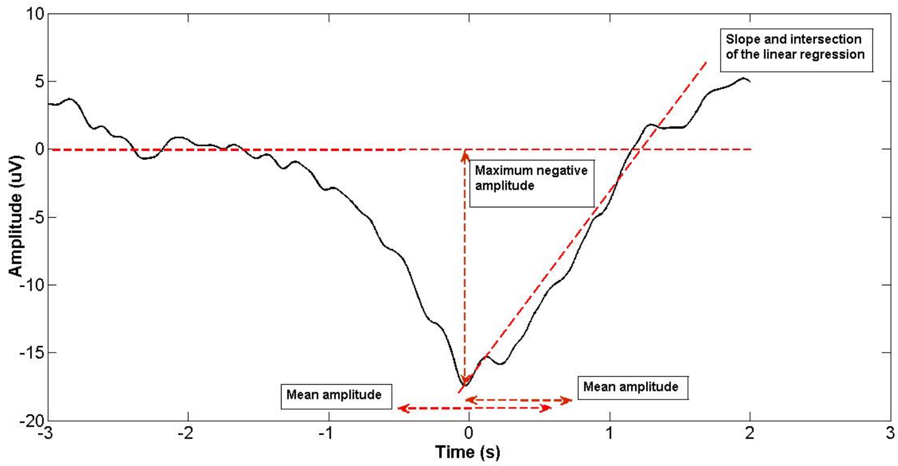

Figure 5.6: *The features were extracted from 2 s before and 1 s after the movement onset. The features are written in the black boxes. Time 0 is the movement onset.*

5.5 Classification

The classification accuracies were obtained for each possible task pair:

- Fast 20% MVC vs. Fast 60% MVC (FL vs. FH).
- Fast 20% MVC vs. Slow 20% MVC (FL vs. SL).
- Fast 20% MVC vs. Slow 60% MVC (FL vs. SH).
- Fast 60% MVC vs. Slow 20% MVC (FH vs. SL).
- Fast 60% MVC vs. Slow 60% MVC (FH vs. SH).
- Slow 20% MVC vs. Slow 60% MVC (SL vs. SH).

The classification accuracies were also obtained for four different filters:

- LLF.
- OSF based on the INP.
- OSF based on the complete MRCP.
- CSP filter.

The results were obtained using an SVM to classify the features extracted from the INP and features extracted from the complete MRCP. Leave-one-out cross-validation was used. Trials which contained EOG amplitudes higher than 100 μV within $\pm$0.5 s of the movement onset were rejected from further classification. In the table below the number of rejected trials per subject are presented as mean$\pm$S.D.

- Fast 20% MVC: 5$\pm$5
- Slow 20% MVC: 8$\pm$9
- Fast 60% MVC: 6$\pm$7
- Slow 60% MVC: 6$\pm$7

SVM

The features were classified using an SVM. The SVM has been reported as a robust classification method with good generalization properties and it has been used in several different tasks including BCI [Farina et al., 2007; Lotte et al., 2007; Schögl et al., 2005].
An SVM is an abstract learning machine which, based on training data, will attempt to generalize and make correct predictions on novel data [Campbell & Ying, 2011]. Training data is a set of input vectors containing the features, each observation (feature vector) is paired with a label of a specific class (e.g. -1 and 1 for two classes). SVMs use a discriminant hyperplane to identify classes (e.g. FH vs. SL). The selected hyperplane is the one that maximizes the margins, based on the distance from the nearest training points (support vectors), which will increase the generalization capabilities (see figure 5.7).

This hyperplane is found by equation 5.8:

$$min_{w,b} \frac{1}{2}||w||^2 \tag{5.8}$$

$$\text{such that } y_i \cdot (w \cdot x_i - b) \geq 1 \tag{5.9}$$

W is the normal vector to the hyperplane (determines the orientation of the discriminant plane), x_i is the data point with the corresponding label y_i and b is the offset of the plane from the origin. Equation 5.8, however, does not account for outliers or errors.

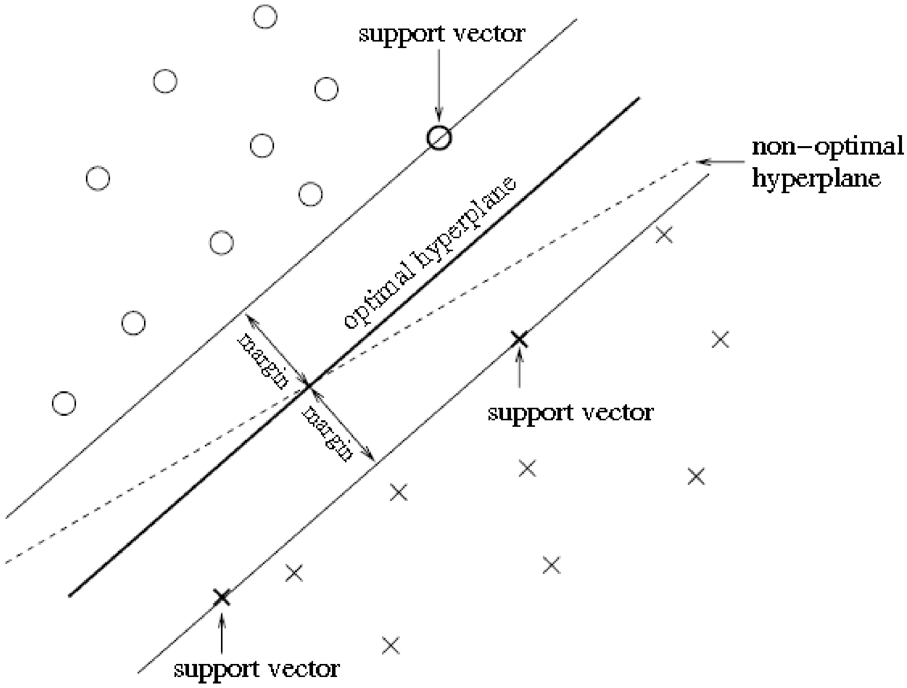

Figure 5.7: *The SVM finds the optimal hyperplane for generalization. The aim is to find the hyperplane which has the largest margins (distance from the hyperplane to the support vectors).The figure is from page 4 in [Lotte et al., 2007]*

Any point falling on the wrong side of the supporting plane is considered an error. To account for outliers and allow errors on the training set, a regularization parameter C is added so the task is to select the hyperplane which will maximize the margin and minimize the error. A nonnegative slack variable z_i is added to each constraint and added to equation 5.8 as a weighted (C) penalty term:

$$min_{w,b}\ \frac{1}{2}||w||^2 + C \cdot \sum_{i=1}^{l} z_i \tag{5.10}$$

$$s.t.\ \ y_i \cdot (w \cdot x_i - b) + z_i \geq 1 \text{ and } z_i \geq 0 \ \ i = 1,..,m \tag{5.11}$$

For more detail about SVMs see [Campbell & Ying, 2011] and [Müller et al., 2001].

5.6 Detection

This section is based on the work of [Niazi et al., 2011]. This part of the study served to investigate the true positive rate (TPR, %), the number of false positive (FP) detections in each task and the latency of the detection compared to the movement onset. These indicators of the detection performance were evaluated for two different spatial filtering techniques; OSF based on the INP and LLF. After the surrogate channel was obtained from the spatial filtering, it was downsampled to 20 Hz to decrease the computational load. A subject specific template of the INP was extracted from the average of all trials and tasks (see figure 5.8). The template was matched to the surrogate channel to detect the movement intention.

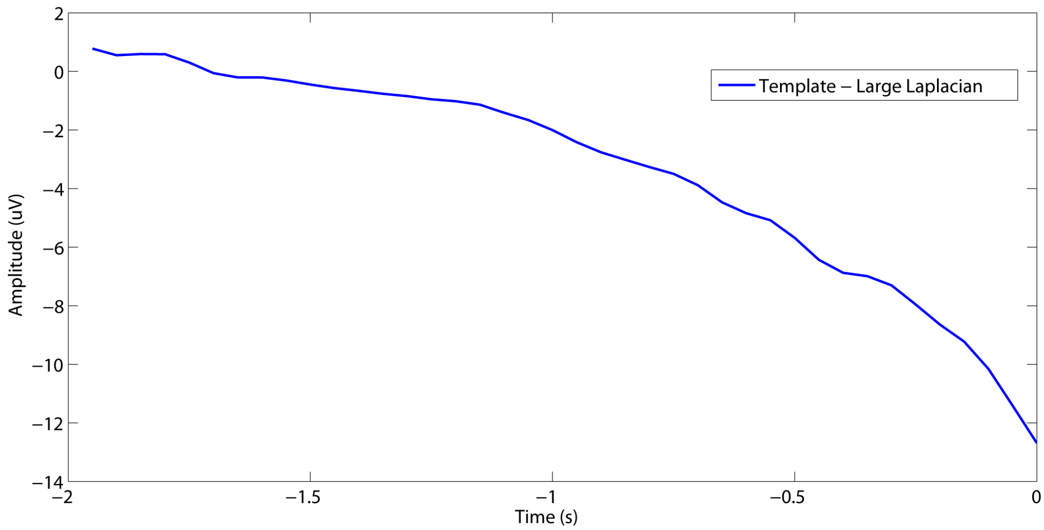

Figure 5.8: *Subject specific template. The template was extracted from the average of all trials and tasks.*

For detection of a movement intention, a receiver operating characteristic (ROC) curve was obtained from the training data (test: 1 task, training: remaining tasks). The detector decision was based on the likelihood ratio method (Neyman Pearson lemma). The likelihood ratio (threshold) was calculated (2 s sliding window shifted with 100 ms) between the template and the training data. The threshold was selected on the midpoint of the turning phase of the ROC curve to obtain a balance between the TPR and the number of FP detections. A threshold for EOG was also determined from the training data. A movement (or detection) was found in the testing set when two out of three consecutive windows crossed the threshold obtained from the training set and the threshold for EOG was not exceeded.

5.7 System Performance

The system performance was evaluated in two ways; a 4-class system with the four different tasks and a 2-class system with the two tasks that were detected and classified with the highest accuracy. The classification in the 4-class system was done with a multiclass SVM, where the three tasks that were not investigated were merged into one group; then SVM for two classes can be used as in section 5.5. The performance of the 4-class system was evaluated based on the following measures:

- Correct detection AND correct classification.
- Correct detection AND incorrect classification.
- Number of FP detections.

The 4-class system was evaluated for the two types of spatial filters used for detection (OSF based on INP and LLF).

The 2-class system performance was evaluated based on the same measures as the 4-class system. However, only the spatial filter with the best performance was evaluated for the task pair with highest detection and classification accuracies. Two values were obtained for the first and the second measure, e.g.

$$1)\ TPR(\text{Fast 60\% MVC})\cdot CA(\text{Fast 60\% MVC vs Slow 60\% MVC}) \quad (5.12)$$

$$2)\ TPR(\text{Slow 60\% MVC})\cdot CA(\text{Fast 60\% MVC vs Slow 60\% MVC}) \quad (5.13)$$

Where CA is the classification accuracy. The mean value was calculated from the two values in equation 5.12 and 5.13.

PART III

Results

CHAPTER 6

Results

This chapter is divided into three sections. In the first section, Classification, the classification results are presented for each task pair and applied spatial filter. The classification was performed on features extracted from the INP of the MRCP and on features from the INP + reafferent potential. In the second section, Detection, the results related to the detection accuracy are presented. Lastly the results of the System Performance are presented, where two systems are evaluated; a 4-class system and a 2-class system.

6.1 Classification

The classification was performed on two different sets of features; features extracted from the INP (until 100 ms before peak negativity of the MRCP) and the same features + features extracted from the reafferent potential. Different spatial filters where tested; LLF, OSF calculated from the INP, OSF calculated from the INP and reafferent potential and CSP calculated between MRCP and random noise. The classification was performed with SVM for each possible task pair. FL: Fast,20% MVC, FH: Fast,60% MVC, SL: Slow,20% MVC, SH: Slow,60% MVC.

INP

In table 6.1 the results for the classification between the task pairs, with features extracted from INP, are presented. All values are presented as mean±S.D. for the 12 subjects. The greatest classification accuracy was found between FH and SL, followed by FH and SH. The poorest classification accuracy was found between SL and SH. This trend was seen for all of the different spatial filters, for the OSF (MRCP), however, the poorest classification accuracy was found between FL and SH.

The performance of the spatial filters showed that the OSF based on the INP performed slightly better than the LLF and OSF based on the MRCP, the performance of CSP was poor compared to the performance of the other filters.

	LLF	OSF (INP)	OSF (MRCP)	CSP
FL/FH	67±10	67±13	67±15	56±12
FL/SL	71±8	72±8	68±10	59±5
FL/SH	70±10	68±12	63±13	57±8
FH/SL	76±9	79±9	77±11	61±12
FH/SH	76±11	75±14	74±11	60±12
SL/SH	64±7	66±6	65±7	56±7
	Mean(%) ±S.D.	Mean(%) ±S.D.	Mean(%) ±S.D.	Mean(%) ±S.D.

Table 6.1: *Classification accuracy for each task pair and spatial filtering technique. All values are presented as mean±S.D. for the 12 subjects. FL: Fast,20% MVC, FH: Fast,60% MVC, SL: Slow,20% MVC, SH: Slow,60% MVC. The greatest classification accuracy was found between FH and SL and the poorest classification accuracy was found between SL and SH. The OSF (INP) performed slightly better than the LLF and OSF (MRCP). The CSP was poor compared to the other techniques.*

INP and Reafferent Potential

In table 6.2 the results for the classification between the task pairs, with features extracted from the complete MRCP, are presented. All values are presented as mean±S.D. for the 12 subjects. The greatest classification accuracy was found between FH and SL, followed by FH and SH. The poorest classification accuracy was found between the SL and SH. This trend was seen for all spatial filters. By adding features extracted from the reafferent potential the classification accuracy increases with approximately 10 percentage points.

The performance of the spatial filters showed that the LLF performed better than the OSF (INP) and OSF (MRCP), which performed almost the same. The performance of CSP was poor compared to the performance of the other filters.

6.2 Detection

The detection performance was evaluated based on the TPR, the number of FP detections during the experiment and the latency of the detection compared to peak negativity. The duration of the experiment is reported as well. The detection performance was evaluated for the LLF (table 6.3) and OSF based on the INP (table 6.4). All values are presented as mean±S.D. for the 12 subjects.

The detection performance for the LLF yields that the fast tasks (FH and FL) have higher TPRs and lower number of FPs compared to the slow tasks (SH and SL). The highest TPR was obtained for FH and the lowest TPR was obtained for SL. The latencies of the detection were approximately -0.5 s for each task.

	LLF	OSF (INP)	OSF (MRCP)	CSP
FL/FH	76±10	71±14	73±14	63±13
FL/SL	80±8	80±11	79±11	66±8
FL/SH	81±10	77±12	73±12	66±8
FH/SL	86±7	84±11	84±8	74±9
FH/SH	83±8	83±13	84±8	73±13
SL/SH	65±9	67±8	67±8	56±8
	Mean(%) ±S.D.	Mean(%) ±S.D.	Mean(%) ±S.D.	Mean(%) ±S.D.

Table 6.2: *Classification accuracy for each task pair and spatial filtering technique. All values are presented as mean±S.D. for the 12 subjects. FL: Fast,20% MVC, FH: Fast,60% MVC, SL: Slow,20% MVC, SH: Slow,60% MVC. The greatest classification accuracy was found between FH and SL and the poorest classification accuracy was found between SL and SH. The LLF performed better than the OSF (INP) and OSF (MRCP). The CSP was poor compared to the other techniques.*

	TPR (%)	FP	Latency (ms)	Duration (min)
FL	81±14	15±7	-535±171	8±0.6
SL	63±20	16±7	-481±256	11±0.9
FH	85±17	15±8	-511±171	8±0.3
SH	77±20	26±8	-604±215	11±0.9
	Mean ±S.D.	Mean ±S.D.	Mean ±S.D.	Mean ±S.D.

Table 6.3: *Detection performance of the LLF. All values are presented as mean±S.D. for the 12 subjects. FL: Fast,20% MVC, FH: Fast,60% MVC, SL: Slow,20% MVC, SH: Slow,60% MVC. The highest TPR was obtained from FH. The lowest TPR was found for SL. FP is the number of false positive detections in the specific task (duration of the task is reported as well). The latencies are with respect to peak negativity. The movements were detected approximately 0.5 s before the movement onset.*

The detection performance for the OSF (INP) yields that the fast tasks (FH and FL) have higher TPRs and a lower number of FPs compared to the slow tasks (SH and SL). The highest TPR was obtained for FH and the lowest TPR was obtained for SL. The latencies of the detection were approximately -0.5 s for each task.
This is similar to the LLF, however, the performance of the two filters differ in the TPR, where the LLF performs better compared to the OSF. The latencies and number of FPs are approximately the same for the two filters.

6.3 System Performance

The system performance is a combination of the detection and classification for two different systems; a 4-class system and a 2-class system. The detection and classification is only based on the INP and

	TPR (%)	FP	Latency (ms)	Duration (min)
FL	76±20	12±9	-467±268	8±0.6
SL	63±16	20±7	-455±264	11±0.9
FH	84±17	15±8	-431±200	8±0.3
SH	68±20	29±7	-492±315	11±0.9
	Mean ±S.D.	Mean ±S.D.	Mean ±S.D.	Mean ±S.D.

Table 6.4: *Detection performance of the OSF (INP). All values are presented as mean±S.D. for the 12 subjects. FL: Fast,20% MVC, FH: Fast,60% MVC, SL: Slow,20% MVC, SH: Slow,60% MVC. The highest TPR was obtained from FH. The lowest TPR was found for SL. FP is the number of false positive detections in the specific task (duration of the task is reported as well). The latencies are with respect to peak negativity. The movements were detected approximately 0.5 s before the movement onset.*

features extracted from the INP.

4-Class System

The classification (see table 6.5) in the 4-class system was performed with a multiclass SVM. The classification accuracies are quite variable, which is also indicated by a relative high standard deviation. The task with the highest classification accuracy was FH, which was the case for both spatial filters, with OSF being the best. The results are presented as mean±S.D.

	LLF	OSF (INP)
FL	15±21	18±21
SL	16±22	23±24
FH	29±22	32±26
SH	20±17	21±20
	Mean(%) ±S.D.	Mean(%) ±S.D.

Table 6.5: *Classification accuracies for the 4-class system for the LLF and OSF (INP) using multiclass SVM. All values are presented as mean±S.D. for the 12 subjects. FL: Fast,20% MVC, FH: Fast,60% MVC, SL: Slow,20% MVC, SH: Slow,60% MVC. The system performs best for FH and worse for slow movements. The results are quite variable, which is also indicated by a relatively high standard deviation.*

The 4-class system was evaluated from the following measures:

- The probability of correct detection multiplied with the probability of correct classification.
- The probability of correct detection multiplied with the probability of incorrect classification.
- Number of FP detections.

In table 6.6 the results for the 4-class system using LLF is presented, the values are presented as mean±S.D. The system performs worse than chance level, but again the task with the highest combined correct detection and classification accuracy is FH. The results are quite variable, especially for the combination of correct detection and classification.

	Detect(+) AND Classify(+)	Detect(+) AND Classify(-)	FP
FL	13±20	68±17	15±7
SL	11±15	52±20	16±7
FH	27±22	58±15	15±8
SH	14±14	62±22	26±8
	Mean(%) ±S.D.	Mean(%) ±S.D.	Mean ±S.D.

Table 6.6: *System performance of the LLF. The + indicates correct detection/-classification, while - indicates incorrect classification. All values are presented as mean±S.D. for the 12 subjects. FL: Fast,20% MVC, FH: Fast,60% MVC, SL: Slow,20% MVC, SH: Slow,60% MVC. The system performs best for FH and worse for slow movements. The results are quite variable, which is also indicated by a relatively high standard deviation.*

In table 6.7 the results of the 4-class system using OSF are presented (mean±S.D.). Similar results as for the LLF were observed: the system performs worse than chance level, FH has the highest combined correct detection and classification accuracy, and the results are quite variable. The system using OSF performs slightly better than the system using the LLF. Both systems were able to detect the movements quite well, but the poor classification accuracies impeded the overall system performance (see table 6.5).

	Detect(+) AND Classify(+)	Detect(+) AND Classify(-)	FP
FL	15±19	61±17	19±9
SL	13±13	49±20	21±7
FH	27±23	56±15	23±8
SH	13±14	55±22	25±7
	Mean(%) ±S.D.	Mean(%) ±S.D.	Mean ±S.D.

Table 6.7: *System performance of the OSF. The + indicates correct detection/-classification, while - indicates incorrect classification. All values are presented as mean±S.D. for the 12 subjects. FL: Fast,20% MVC, FH: Fast,60% MVC, SL: Slow,20% MVC, SH: Slow,60% MVC. The system performs best for FH and worse for slow movements. The results are quite variable, which is also indicated by a relatively high standard deviation.*

It is clearly seen that the system performance for a 4-class system is really poor, therefore a two-class system was evaluated as well, where the task pair with the best detection and classification performance was evaluated. The task pair with the best performance for detection and classification was *FH vs SH* for the LLF, in this task the torque amplitude was the same (60% MVC, so it only differed in the RTD. The system performance was also investigated for the task pair '*FL vs FH*' when the RTD (fast) was fixed, so 20% MVC was compared to 60% MVC.

2-Class System

The results of the 2-class system (mean±S.D.) are presented in table 6.8. The 2-class system for FH and SH correctly detected and classified the movements 61% of the time, while the 2-class system for FL and FH correctly detected and classified the movements 56% of the time. The overall detection performance was quite high, but again the results are quite variable, which is indicated by the standard deviation. The average duration of the recordings were 19 and 17 minutes respectively. The results are based on 12 subjects.

	Detect(+) AND Classify(+)	Detect(+) AND Classify(-)	FP
FL vs FH	56±16	27±8	29±14
FH vs SH	61±15	20±10	40±11
	Mean(%) ±S.D.	Mean(%) ±S.D.	Mean ±S.D.

Table 6.8: *2-class system performance. Two systems were evaluated: FL vs FH and FH vs SH, the duration of the recordings were on average 17 and 19 minutes respectively. The '+' indicates correct detection/classification, while '-' indicates incorrect classification. All values are presented as mean±S.D. for the 12 subjects. FL: Fast,20% MVC, FH: Fast,60% MVC and SH: Slow,60% MVC.*

PART IV

Synthesis

CHAPTER 7

Discussion

The discussion is divided into five sections. Initially the findings of this study are summarized. The following three sections go into detail about the detection performance, classification accuracies and overall system performance. Finally methodological considerations are outlined.

7.1 Summary

The aim of the study had three purposes; detecting MRCPs from different tasks, classifying MRCPs from different tasks and evaluating a simulated BCI when detection and classification were combined.
The TPR of detections was higher for fast movements compared to slow movements (see table 6.3), ranging from 85±17% TPR (*fast 60% MVC*) to 63±20% TPR (*slow 20% MVC*) using the LLF.
The task pairs with different RTD had the highest classification accuracies and fixed RTD had the lowest classification accuracies. The range was from 79±9% (*fast 60% MVC vs slow 60% MVC* and *fast 60% MVC vs slow 20% MVC*) to 66±6% (*slow 20% MVC vs slow 60% MVC*) for the OSF.
The overall system performance for a 4-class system was evaluated, but with a performance below chance level, the 4-class system was reduced to a 2-class system. The 2-class system was evaluated for task pairs; where the torque amplitude was fixed at 60% MVC, and where the RTD was fixed at fast RTD. The systems correctly detected and classified the movements 61±15% and 56±16% of the time respectively using LLF.
This study was the first to investigate the 4-class and 2-class system performance using different parameters of MRCP as control signals.

7.2 Detection

The detection performance was investigated for the LLF and OSF with LLF performing slightly better than OSF. This is contradicting to the findings of [Niazi et al., 2011] where OSF performed slightly better than the LLF. The reason for the slightly worse performance of the OSF in this study could be due to the fact that the OSF was based on

trials from four different tasks, which are not morphologically similar.
Both filters had the highest TPR for fast movements (20% MVC and 60% MVC) and slow movements performed at 60% MVC. This is most likely related to an increased SNR in these tasks (see figure 5.4), because the amplitude of the MRCP is modulated by RTD and torque level (see section 3.2). The TPR was impeded by EOG, because EOG artifacts surrounding the movement onset blocked the detection of movements (due to the EOG threshold). Approximately 25 trials in total were contaminated with EOG around the movement onset per subject.
Another factor affecting the detection performance was the detection threshold. It was based on a trade-off between the TPR and number of FP detections. By decreasing the threshold the TPR will increase, but so will the number of FP detections.

Besides the TPR and number of FP detections, the detection performance was evaluated based on the detection latency to test if it was possible to trigger a stimulator so the afferent feedback would coincide with the MP [Mrachacz-Kersting et al., 2012]. The movements were detected approximately 0.5 s before the movement onset which is more than enough time to start a stimulator and make the afferent feedback coincide with the MP. The movements were detected much earlier compared to the findings of [Niazi et al., 2011], an explanation could be that the movements in this study were cue-based on the contrary to self-paced movement in [Niazi et al., 2011]. Cue-based movements have a longer INP compared to that of self-paced movements [Jankelowitz & Colebatch, 2002] and therefore a match with the template may exceed the threshold much earlier than in the self-paced mode.

7.3 Classification

Overall the results for classification accuracies of task pairs are in agreement with what has previously been reported [Farina et al., 2007; Gu, Nascimento, et al., 2009; Nascimento & Farina, 2008]. However, the features that were used in this study, differ from those previously reported. The performance of the LLF and OSF for classification were much higher compared to the CSP filter for the current amount of training data (in [Blankertz, Losch, et al., 2008] 420 trials of motor imagery were used as training data). The CSP filter was also implemented with signal and noise as the two conditions [Niazi et al., 2011], which is in contrast to the traditional way of implementing it, where the variance is maximized between between two classes of signals [Blankertz, Losch, et al., 2008] (e.g. left hand movements and right hand movements). However, it was not feasible to implement

the CSP filter in that way for detection purposes. The reason why the CSP filtered data had really low classification accuracies can be seen in figure 5.3, the morphology of the signal was changed and therefore the extracted features could not be classified correctly.
For all spatial filters, the two task pairs that had the highest classification accuracies were *fast 60% MVC vs slow 60% MVC* and *fast 60% MVC vs slow 20% MVC*. This result was also expected, since RTD has been reported in several studies to affect the MRCP more than the torque amplitude (e.g. [Brunia & Vingerhoets, 1980; Nascimento et al., 2005, 2006]). Even though task pairs with different levels of RTD had higher classification accuracies, the torque amplitude could also be discriminated for fast RTD which is in line with the findings of [Nascimento et al., 2005].

The classification accuracies were also investigated when information from the reafferent potential was included. The information from the reafferent potential led to an increase of approximately 10 percentage points. The reafferent potential holds additional discriminative information about a movement, especially for different levels of RTD [Nascimento et al., 2005].

7.4 System Performance

The system performance of the 4-class system was below chance level. This was mainly due to very low classification accuracies when using a multiclass SVM (because of low separability of the four classes). The low classification accuracies are related to the huge variability that is observed in single-trial EEG analysis [Wolpaw et al., 2002]. The tasks were not as easily discriminated compared to the 2-class system, which was only a binary selection instead of a selection of four possible choices. The task *fast 60% MVC* had the best performance due to relatively high classification accuracies and TPR, a likely reason for this is the higher SNR present in these trials compared to the others.
Based on the results for the 4-class system performance, and especially the classification accuracies with multiclass SVM (table 6.5), the number of classes was reduced to obtain better system performance. The 4-class system was reduced and investigated for two 2-class systems using *fast 60% MVC vs slow 60% MVC* and *fast 60% MVC vs fast 20% MVC*, where the torque and RTD was fixed respectively. *Slow 60% MVC* was selected instead of *Slow 20% MVC* due to a higher TPR, 77±20% and 63±20% respectively. When the torque was fixed the system correctly detected and classified the movements 61±15% of the time and detected movements correctly but misclassified these 20±10% of the time. With RTD fixed 56±16% of the time the system correctly detected and classified the movements, the mis-

classification of detected movements was 27±8%. The detection performance is reasonably high, but it is the classification accuracy that impedes the overall system performance. It is important to improve the classification accuracy to be able to differentiate between different movements so appropriate feedback can be given to the subject. In [Shea & Kohl, 1991] it is stated that introducing task variability in a session will improve functional performance in subsequent sessions. Another benefit of having more classes (or differentiating between movements) is that it increases the generalization of learning new tasks [Krakauer, 2006]. In rehabilitation generalization is important. Training one task repeatedly in the clinic may lead to improved performance in that particular task, but it may not transfer to more general tasks in the subject's daily living outside the clinic [Krakauer, 2006].

7.5 Methodological Considerations

In this study the signals were processed offline and then simulated in a pseudo-online fashion. Based on the signal processing techniques, feature extraction and classification, online detection and classification is possible, which has been proven by [Niazi et al., 2012]. Online detection and classification for two or more classes still need to be verified through online studies.

A problem that was not addressed in this study is to find the time from when the algorithm detects a movement until the actual time of peak negativity. The classification accuracies were calculated from features extracted from the initial negative phase until 100 ms before peak negativity. If the detection of a movement intention occurs 0.5 s before the movement onset, then there are 400 ms less of the INP to use in the feature extraction; this will make the system performance worse.

Depending on the processing time of the BCI system it should also be investigated if it is possible to include more of the INP (move closer to peak negativity) in the feature extraction to improve the classification accuracies, but the constraint is that the system must trigger the external device so the afferent feedback will coincide with MP [Mrachacz-Kersting et al., 2012].

The features used in this study were extracted from the time domain, but also the DWT marginals were used as features in pilot testing, but good results were not obtained on the contrary to [Farina et al., 2007], which could be explained by the fact that no optimization was performed on the mother wavelet that was used in the analysis. If DWT marginals are used the wavelet optimization should be done for each subject. Other features that should be investigated in combination with those from the MRCP are features extracted from the frequency domain such as event-related desynchronization amplitude.

A greater knowledge of the MRCP, generators and morphology, may provide information of better features. The features should be insensitive to the trial-to-trial variability and the changes from fatigue and other spontaneous variations [Daly & Wolpaw, 2008; Wolpaw et al., 2002].
Besides the features, EOG affect the system performance as well (see section 7.2). Approximately 25 trials were contaminated with EOG around the movement onset per subject out of 200; this impedes the detection and the overall system performance. The number of EOG contaminated trials may be reduced by increasing the distance between the subject and the screen or making the animation smaller (based on subject feedback). The subjects were instructed to focus their gaze at a specific point on the screen, but they reported that it was difficult, especially for the slow movements at 20% MVC, because they had to correct the torque level all the way up to the desired torque level. When 25 out of 200 trials will not be detected (due to the EOG threshold) more than 50 trials have to be performed per task to reach the number of trials needed to induce plasticity [Mrachacz-Kersting et al., 2012]. With the current system performance of 61±15%, 82 trials have to be performed to reach 50 correctly detected and classified movements. This number can be reduced by improving the system performance either by system calibration or subject training [Blankertz, Losch, et al., 2008; Kübler et al., 2005; Wolpaw et al., 2002].

CHAPTER 8

Conclusion

This chapter concludes on the aim stated in chapter 4, where the classification and detection performance were to be analyzed as well as the system performance.

The first part of the aim was to evaluate the classification accuracies between tasks pairs. Overall the task pairs could be discriminated using the specified features, but the tasks involving FH and slow tasks (SL and SH) showed the highest classification accuracies (76±9% for the LLF and 79±9% for the OSF). It can be concluded that the tasks where the RTD was different had higher classification accuracies compared to the tasks where the RTD was fixed. For fixed RTDs the highest classification accuracies were found when the movements were fast. When including features from the reafferent potential the classification accuracies increased by approximately 10 percentage points.

The second part of the aim demonstrates that movements can be detected from the INP approximately 0.5 s before the movement onset. Based on the TPR it can be concluded that the detection performance is better for fast compared to slow movements, but also for high compared to low torque amplitudes.

From the results of the system performance it can be concluded that a 4-class system cannot be used at the moment, and it should be reduced to a 2-class system instead, using FH and SH. The 2-class system correctly detected and classified the movements 61±15% of the time and 20±10% of the time the movements were detected but misclassified. The number of FP detections was on average two per minute.

References

Abbruzzese, G., Assini, A., Buccolieri, A., Marchese, R., & Trompetto, C. (1999). Changes of intracortical inhibition during motor imagery in human subjects. *Neuroscience Letters, 263*, 113-116.

Abraham, W. C., Logan, B., Greenwood, J. M., & Dragunow, M. (2002). Induction and experience-dependent consolidation of stable long-term potentiation lasting months in the hippocampus. *The Journal of Neuroscience, 21*, 9626-9634.

Birbaumer, N., & Cohen, L. G. (2007). Brain computer interfaces: communication and restoration of movement in paralysis. *J Physiol, 579.3*, 621-636.

Blankertz, B., Losch, F., Krauledat, M., Dornhege, G., Curio, G., & Müller, K. R. (2008, October). The berlin brain–computer interface: Accurate performance from first-session in bci-naive subjects. *IEEE Transactions on Biomedical Engineering, 55*(10), 2452-2462.

Blankertz, B., Tomioka, R., Lemm, S., Kawanabe, M., & Müller, K.-R. (2008). Optimizing spatial filters for robust eeg single-trial analysis. *IEEE Signal Processing Magazine, 25*, 41-56.

Bliss, T. V. P., Collingridge, G. L., & Morris, R. G. M. (2003). Long-term potentiation: enhancing neuroscience for 30 years. *Philos Trans R Soc, 358*, 607–611.

Borda, R. P. (1970). The effect of altered drive states on the contingent negative variation (cnv) in rhesus monkeys. *Electroenceph. clin. Neurophysiol.,, 29*, 173–180.

Brunia, C. H. M. (2003). The bereitschaftpotential - movement-related cortical potentials. In M. Jahanshahi & M. Hallett (Eds.), (p. 207-227). Kluwer Academic/Plenum Publishers, New York.

Brunia, C. H. M., & Vingerhoets, A. J. J. M. (1980). Cnv and emg preceding a plantar flexion of the foot. *Biological Psychology, 11*, 181-191.

Buonomano, D. V., & Merzenich, M. M. (1998). Cortical plasticity: From synapses to maps. *Annu. Rev. Neurosci, 21*, 149–86.

Byrd, R. H., & Nocedal, J. (1989). A tool for the analysis of quasi-newton methods with application to unconstrained minimization. *Society for Industrial and Applied Mathematics, 26*, 727-739.

Campbell, C., & Ying, Y. (2011). Learning with support vector machines. In R. J. Brachman & T. Dietterich (Eds.), (p. 1-21). Morgan & Claypool Publishers.

Chouinard, P. A., Werf, Y. D. V. D., Leonard, G., & Paus, T. (2003). Modulating neural networks with transcranial magnetic stimulation applied over the dorsal premotor and primary motor cortices. *J Neurophysiol*, *90*, 1071-1083.

Connor, W. H., & Lang, P. J. (1969). Cortical slow wave and cardiac rate responses in stimulus orientation and reaction time conditions. *Journal of Experimental Psychology*, *82*, 310-320.

Cooke, S. F., & Bliss, T. V. P. (2006). Plasticity in the human central nervous system. *Brain*, *129*, 1659-1673.

Cooper, R., McCallum, W. C., & Cornthwaite, S. P. (1989). Slow potential changes related to the velocity of target movement in a tracking task. *EEG Clin Neurophysiol*, *72*, 232-239.

Crammond, D. J., & Kalaska, J. F. (2000). Prior information in motor and premotor cortex: Activity during the delay period and effect on pre-movement activity. *J Neurophysiol*, *84*, 986-1005.

Cui, R., Egkher, A., Huter, D., Lang, W., Lindinger, G., & Deecke, L. (2000). High resolution spatiotemporal analysis of the contingent negative variation in simple or complex motor tasks and a non-motor task. *Clinical Neurophysiology*, *111*, 1847-1859.

Daly, J. J., Cheng, R., Rogers, J., Litinas, K., Hrovat, K., & Dohring, M. (2009). Feasibility of a new application of noninvasive brain computer interface (bci): A case study of training for recovery of volitional motor control after stroke. *Journal of neurologic physical therapy*, *33*(4), 203-211.

Daly, J. J., & Wolpaw, J. R. (2008). Brain-computer interfaces in neurological rehabilitation. *The Lancet Neurology*, *7, Issue 11*, 1032 - 1043.

Dastmalchi, S. (2003). *Functional brain imaging: extracting temporal responses of multiple cortical areas from multi-focal visual evoked potentials*. Unpublished doctoral dissertation, University of California, Berkeley.

Decety, J. (1996). The neurophysiological basis of motor imagery. *Behav Brain Res*, *77*, 45-52.

Deiber, M.-P., Ibanez, V., Sadato, N., & Hallett, M. (1996). Cerebral structures participating in motor preparation in humans: A positron emission tomography study. *Journal of Neurophysiology*, *75*(1), 233-247.

Donchin, E., Otto, D., Gerbrandt, L. K., & Pribram, K. H. (1971). While a monkey waits: electrocortical events recorded during the foreperiod of a reaction time study. *Electroenceph. clin. Neurophysiol*, *31*, 115–127.

Everaert, D. G., Thompson, A. K., Chong, S. L., & Stein, R. B. (2009). Does functional electrical stimulation for foot drop strengthen corticospinal connections? *Neurorehabilitation and Neural Repair*, *24*(2), 168-177.

Fadiga, L., Buccino, G., Craighero, L., Fogassi, L., Gallese, V., & Pavesi, G. (1998). Corticospinal excitability is specifically modulated by motor imagery: a magnetic stimulation study. *Neuropsychologia*, *37*, 147-158.

Fang, Y., Siemionow, V., Sahgal, V., Xiong, F., & Yue, G. H. (2004). Distinct brain activation patterns for human maximal voluntary eccentric and concentric muscle actions. *Brain Research*, *1023*, 200-212.

Farina, D., Nascimento, O. F. do, Lucas, M.-F., & Doncarli, C. (2007). Optimization of wavelets for classification of movement-related cortical potentials generated by variation of force-related parameters. *Journal of Neuroscience Methods*, *162*, 357–363.

Gomez-Rodriguez, M., Peterst, J., Hint, J., Scholkoprt, B., Gharabaghi, A., & Grosse-Wentrupt, M. (2010). Closing the sensorimotor loop: Haptic feedback facilitates decoding of arm movement imagery. *IEEE, Systems Man and Cybernetics (SMC)*, 121-126.

Grafton, S. T., Fagg, A. H., & Arbib, M. A. (1998). Dorsal premotor cortex and conditional movement selection: A pet functional mapping study. *J Neurophysiol*, *79*, 1092-1097.

Grünewald, G., & Grünewald-Zuberbier, E. (1983). Tutorials in event-related potentials research: Endogenous components. In A. W. K. Gaillard & W. Ritter (Eds.), (p. 311-327). North-Holland Publishing Company - Amsterdam.

Grosse-Wentrup, M., Mattia, D., & Oweiss, K. (2011). Using brain-computer interfaces to induce neural plasticity and restore function. *Journal of Neural Engineering*, *8*.

Gu, Y., Dremstrup, K., & Farina, D. (2009). Single-trial discrimination of type and speed of wrist movements from eeg recordings. *Clinical Neurophysiology*, *120*, 1596-1600.

Gu, Y., Farina, D., Murguialday, A. R., Dremstrup, K., Montoya, P., & Birbaumer, N. (2009). Offline identification of imagined speed of wrist movements in paralyzed ALS patients from single-trial EEG. *frontiers in NEUROSCIENCE*, *3*, 1-7.

Gu, Y., Nascimento, O. F. do, Lucas, M.-F., & Farina, D. (2009). Identification of task parameters from movement-related cortical potentials. *Med Biol Eng Comput*, *47*, 1257-1264.

Guyton, A. C., & Hall, J. E. (2005). *Textbook of medical physiology, 11th edition.* Saunders/Elsevier.

Hamano, T., Lüders, H. O., Ikeda, A., Collura, T. F., Comair, Y. G., & Shibasaki, H. (1997). The cortical generators of the contingent negative variation in humans: a study with subdural electrodes. *Electroencephalography and clinical Neurophysiology*, *104*, 257–268.

Hebb, D. O. (1949). *The organization of behavior: A neuropsychological theory.* John Wiley & Sons Inc.

Hultin, L., Rossini, P., Romani, G., Högstedt, P., Tecchio, F., & Pizzella, V. (1996). Neuromagnetic localization of the late component of the contingent negative variation. *Electroencephalography and clinical Neurophysiology*, *98*, 435-448.

Ikeda, A., Lüders, H. O., Collura, T. F., Morris, R. B. H. H., Hamano, T., & Shibasaki, H. (1996). Subdural potentials at orbitofrontal and mesial prefrontal areas accompanying anticipation and decision making in humans: a comparison with bereitschaftspotential. *Electroenceph clin Neurophysiol*, *98*(3), 206-212.

Ikeda, A., Shibasaki, H., Kaji, R., Terada, K., Nagamine, T., Honda, M., et al. (1997). Dissociation between contingent negative variation (cnv) and bereitschaftspotential (bp) in patients with parkinsonism. *Electroencephalography and clinical Neurophysiology*, *102*, 142- 151.

Ikeda, A., Shibasaki, H., Nagamine, T., Terada, K., Kaji, R., Fukuyama, H., et al. (1994). Dissociation between contingent negative variation and bereitschaftspotential in a patient with cerebellar efferent lesion. *Electroencephalography and clinical Neurophysiology*, *90*, 359-364.

Jankelowitz, S. K., & Colebatch, J. G. (2002). Movement-related potentials associated with self-paced, cued and imagined arm movements. *Exp Brain Res*, *147*, 98-107.

Jenkins, W. M., Merzenich, M. M., Ochs, M. T., Allard, T., & Guíc-Robles, E. (1990). Functional reorganization of primary somatosensory cortex in adult owl monkeys after behaviorally controlled tactile stimulation. *Journal of Nerophysiology*, *63*, 82-104.

Jochumsen, M., & Jensen, A. Ågård. (2011). *Inducing plasticity in the human central nervous system by using a brain-computer interface with different feedback modalities.*

Kawanabe, M., Vidaurre, C., Blankertz, B., & Müller, K.-R. (2009). A maxmin approach to optimize spatial filters for eeg single-trial classification. *Bio-Inspired Systems: Computational and Ambient Intelligence (LNCS 5517)*, 674-682.

Kübler, A., Nijboer, F., Mellinger, J., Vaughan, T., Pawelzik, H., Schalk, G., et al. (2005). Patients with als can use sensorimotor rhythms to operate a brain-computer interface. *Neurology*, *64*(10), 1775-1777.

Khaslavskaia, S., Ladouceur, M., & Sinkjaer, T. (2002). Increase in tibialis anterior motor cortex excitability following repetitive electrical stimulation of the common peroneal nerve. *Exp Brain Res*, *145*, 309-315.

Kimberley, T. J., Lewis, S. M., Dorsey, E. J. A. A. L., Lojovich, J. M., & Carey, J. R. (2004). Electrical stimulation driving functional improvements and cortical changes in subjects with stroke. *Exp Brain Res*, *154*, 450-460.

Klem, G. H., Lüders, H. O., Jasper, H. H., & Elger, C. (1999). The ten-twenty electrode system of the international federation. *Electroencephalogr Clin Neurophysiol Suppl*, *52*, 3-6.

Krakauer, J. W. (2006, February). Motor learning: its relevance to stroke recovery and neurorehabilitation. *Current Opinion in Neurology*, *19*(1), 84-90.

Kurata, K., & Hoffman, D. S. (1994). Differential effects of muscimol microinjection into dorsal and ventral aspects of the premotor cortex of monkeys. *Journal of Neurophysiology*, *71*(3), 1151-1164.

Kurata, K., & Wise, S. (1988). Premotor and supplementary motor cortex in rhesus monkeys: neuronal activity during externally- and internally-instructed motor tasks. *Exp Brain Res*, *72*, 237-248.

Langhorne, P., Coupar, F., & Pollock, A. (2009). Motor recovery after stroke: a systematic review. *Lancet Neurol*, *8*, 741-54.

Liepert, J., Bauder, H., Miltner, W. H. R., Taub, E., & Weiller, C. (2000). Treatment-induced cortical reorganization after stroke in humans. *Stroke*, *31*, 1210-1216.

Lotte, F., Congedo, M., Lécuyer, A., Lamarche, F., & Arnaldi, B. (2007). A review of classification algorithms for eeg-based brain–computer interfaces. *J. Neural Eng*, *4*, R1-R13.

Lu, M.-K., Arai, N., Tsai, C.-H., & Ziemann, U. (2011). Movement related cortical potentials of cued versus self-initiated movements: Double dissociated modulation by dorsal premotor cortex versus supplementary motor area rtms. *Human Brain Mapping*, *00*, 000-000.

Mackay, J., & Mensah, G. A. (2004). *The atlas of heart disease and stroke* (H. Ann, Ed.). World Health Organization.

Malenka, R. C., & Bear, M. F. (2004). Ltp and ltd: An embarrassment of riches. *Neuron*, *44*, 5-21.

Mallat, S. G. (1989). A theory of multiresolution signal decomposition: the wavelet representation. *IEEE Trans Pattern Anal Mach Intell, 11*(7), 674-693.

Matsumoto, R., Ikeda, A., Ohara, S., Matsuhashi, M., Baba, K., Yamane, F., et al. (2003). Motor-related functional subdivisions of human lateral premotor cortex: epicortical recording in conditional visuomotor task. *Clinical Neurophysiology 114 (2003) 1102–1115, 114*, 1102-1115.

McSherry, J. W., & Borda, R. P. (1973). The intracortical distribution of the cnv in rhesus monkey. *Electroenceph. clin. Neurophysiol., 33*, 69-74.

Meng, F., Tong, K. yu, Chan, S. tak, Wong, W. wa, Lui, K. him, Tang Xiaorong Gao, K. wing, et al. (2008). Bci-fes training system design and implementation for rehabilitation of stroke patients. *IEEE*, 4103 - 4106.

Merzenich, M. M., Kaas, J. H., Wall, J. T., Sur, M., Nelson, R. J., & Felleman, D. J. (1983). Progression of change following median nerve section in the cortical representation of the hand in areas 3b and 1 in adult owl and squirrel monkeys. *Neuroscience, 10*, 639-665.

Merzenich, M. M., & Sameshima, K. (1993). Cortical plasticity and memory. *Current Opinion in Neurobiology, 3*, 187-196.

Müller, K.-R., Mika, S., Rätsch, G., & Schölkopf, K. T. B. (2001, March). An introduction to kernel-based learning algorithms. *IEEE Transactions on Neural Networks, 12*(2), 181-201.

Mrachacz-Kersting, N., Fong, M., Murphy, B. A., & Sinkjaer, T. (2007). Changes in excitability of the cortical projections to the human tibilalis anterior after paired associative stimulation. *Journal of Neurophysiology, 97*, 1951-1958.

Mrachacz-Kersting, N., Kristensen, S. R., Niazi, I. K., & Farina, D. (2012). Precise temporal association between cortical potentials evoked by motor imagination and afference induces cortical plasticity. *The Journal of Physiology, 590*(7), 1669-1682.

Mushiake, H., Inase, M., & Tanji, J. (1991). Neuronal activity in the primate premotor, supplementary, and precentral motor cortex during visually guided and internally determined sequential movements. *Journal of Neurophysiology, 66*(3), 705-718.

Nagai, Y., Critchley, H., Featherstone, E., Fenwick, P., Trimble, M., & Dolan, R. (2004). Brain activity relating to the contingent negative variation: an fmri investigation. *NeuroImage, 21*, 1232-1241.

Nascimento, O. F. do, & Farina, D. (2008). Movement-related cortical potentials allow discrimination of rate of torque development in imaginary isometric plantar flexion. *IEEE Transactions on Biomedical Engineering*, *55*(11), 2675-2678.

Nascimento, O. F. do, Nielsen, K. D., & Voigt, M. (2005). Relationship between plantar-flexor torque generation and the magnitude of the movement-related potentials. *Exp Brain Res*, *160*, 154-165.

Nascimento, O. F. do, Nielsen, K. D., & Voigt, M. (2006). Movement-related parameters modulate cortical activity during imaginary isometric plantar flexions. *Exp Brain Res*, *171*, 78-90.

Niazi, I. K., Jiang, N., Tiberghien, O., Nielsen, J. F., Dremstrup, K., & Farina, D. (2011). Detection of movement intention from single-trial movement-related cortical potentials. *Journal of Neural Engineering*, *8*(6).

Niazi, I. K., Jiang, N. M.-K. A. N., Dremstrup, K., & Farina, D. (2012). Peripheral electrical stimulation triggered by self-pace detection of motor intention enhances motor evoked potentials. *IEEE Transactions on Neural Systems and Rehabilitation Engineering*(99), 1-10.

Nudo, R. J. (2006). Mechanisms for recovery of motor function following cortical damage. *Current Opinion in Neurobiology*, *16*, 638-644.

Pascual-Leone, A., Cammarota, A., Wassermann, E. M., Brasil-Neto, J. P., Cohen, L. G., & Hallett, M. (1993). Modulation of motor cortical outputs to the reading hand of braille readers. *Ann. Neurol.*, *34*, 33-37.

Pascual-Leone, A., Dang, N., Cohen, L. G., Brasil-Neto, J. P., Cammarota, A., & Hallett, M. (1995). Modulation of muscle responses evoked by transcranial magnetic stimulation during the acquisition of new fine motor skills. *J. Neurophysiol*, *74*, 1037-1045.

Pearce, A. J., Thickbroom, G. W., Byrnes, M. L., & Mastaglia, F. L. (2000). Functional reorganisation of the corticomotor projection to the hand in skilled racquet players. *Exp. Brain Res*, *130*, 238–243.

Polikar, R. (2006, November). *The engineer's ultimate guide to wavelet analysis: The wavelet tutorial.* (Course material from a course in Joint-Time Frequency Analysis)

Popovic, D., & Sinkjær, T. (2000). *Control of movement for the physically disabled : control for rehabilitation technology.* Aalborg : Center for Sensory-Motor Interaction, Aalborg University.

Ray, W. J., Slobounov, S., Mordkoff, J. T., Johnston, J., & Simon, R. F. (2000). Rate of force development and the lateralized readiness potential. *Psychophysiology*, *37*, 757-765.

Rich, M. M., & Wenner, P. (2006). Sensing and expressing homeostatic synaptic plasticity. *TRENDS in Neurosciences*, *30*, 119-125.

R. Millán, J. d., Rupp, R., Müller-Putz, G. R., Murray-Smith, R., Giugliemma, C., Tangermann, M., et al. (2010). Combining brain–computer interfaces and assistive technologies: state-of-the-art and challenges. *frontiers in NEUROSCIENCE*, *4*, 1-15.

Rohrbaugh, J., & Gaillard, A. W. K. (1983). Tutorials in event-related potentials research: Endogenous components. In A. W. K. Gaillard & W. Ritter (Eds.), (p. 269-310). North-Holland Publishing Company - Amsterdam.

Rohrbaugh, J. W., Syndulko, K., & Lindsley, D. B. (1976). Brain wave components of the contingent negative variation in humans. *American Association for the Advancement of Science*, *191*(4231), 1055-1057.

Romero, D. H., Lacourse, M. G., Lawrence, K. E., Schandler, S., & Cohen, M. J. (2000). Event-related potentials as a function of movement parameter variations during motor imagery and isometric action. *Behavioural Brain Research*, *117*, 83-96.

Ruchkin, D. S., Johnson, R. J., Canoune, H., & Ritter, W. (1992). Distinctions and similarities among working memory processes: an event-related potential study. *Cognitive Brain Research*, *1*, 53-66.

Schalk, G., Wolpaw, J. R., McFarland, D. J., & Pfurtscheller, G. (2000). Eeg-based communication and control: presence of error potentials. *Clin Neurophysiol*, *111*, 2138-2144.

Schögl, A., Lee, F., Bischof, H., & Pfurtscheller, G. (2005). Characterization of four-class motor imagery eeg data for the bci-competition 2005. *J. Neural Eng.*, *2*, 14-22.

Shea, C. H., & Kohl, R. M. (1991). Composition of practice: Influence on the retention of motor skills. *Res Q Exerc Sport*, *62*, 187-195.

Shibasaki, H., & Hallett, M. (2006). What is the bereitschaftspotential? *Clinical Neurophysiology*, *117*, 2341-2356.

Simon, S. R., Meunier, M., Piettre, L., Berardi, A. M., Segebarth, C. M., & Boussaoud, D. (2002). Spatial attention and memory versus motor preparation: Premotor cortex involvement as revealed by fmri. *J Neurophysiol*, *88*, 2047-2057.

Slobounov, S., Hallett, M., & Newell, K. M. (2004). Perceived effort in force production as reflected in motor-related cortical potentials. *Clinical Neurophysiology*, *115*, 2391-2402.

Slobounov, S., Johnston, J., Chiang, H., & Ray, W. (2002). Movement-related eeg potentials are force or end-effector dependent: evidence from a multi-finger experiment. *Clinical Neurophysiology*, *113*, 1125-1135.

Slobounov, S., Rearick, M., & Chiang, H. (2000). Eeg correlates of finger movements as a function of range of motion and pre-loading conditions. *Clinical Neurophysiology*, *111*, 1997-2007.

Slobounov, S. M., & Ray, W. J. (1998). Movement-related potentials with reference to isometric force output in discrete and repetitive tasks. *Exp Brain Res*, *123*, 461-473.

Sörnmo, L., & Laguna, P. (2005). *Bioelectrical signal processing in cardiac and neurological applications* (L. Sörnmo & P. Laguna, Eds.). Elsevier Academic Press.

Stefan, K., Kunesch, E., Cohen, L. G., Benecke, R., & Classen, J. (2000). Induction of plasticity in the human motor cortex by paired associative stimulation. *Brain*, *123*, 572-584.

Stinear, C. M., Byblow, W. D., Steyvers, M., Levin, O., & Swinnen, S. P. (2006). Kinesthetic, but not visual, motor imagery modulates corticomotor excitability. *Exp Brain Res.*, *168*, 157-164.

Tecce, J. J. (1972). Contingent negative variation (cnv) and psychological processes in man. *Psychol. Bull.*, *77*, 73-108.

Thickbroom, G. W. (2007). Transcranial magnetic stimulation and synaptic plasticity: experimental framework and human models. *Exp Brain Res*, *180*, 583-593.

Volodin iStockphoto/Andrey. (2010, January). ScienceDaily. Available from `http://www.sciencedaily.com/releases/2010/01/100125122101.htm`

Walter, W., Cooper, R., Aldridge, V., McCallum, W., & Winter, A. (1964). Contingent negative variation: an electric sign of sensori-motor association and expectancy in the human brain. *Nature*, *203*, 380-384.

Weiss, T., Hansen, E., Rost, R., Beyer, L., Merten, F., Nichelmann, C., et al. (1994). Mental practice of motor skills used in post-stroke rehabilitation has own effects on central nervous activation. *Intern. J. Neuroscience*, *78*, 157-166.

Wise, S. P., Boussaoud, D., Johnson, P. B., & Caminiti, R. (1997). Premotor and parietal cortex: Corticocortical connectivity and combinatorial computations. *Annu. Rev. Neurosci.*, *20*, 25-42.

Wolpaw, J. R., Birbaumer, N., McFarland, D. J., Pfurtscheller, G., & Vaughan, T. M. (2002). Brain computer interfaces for communication and control. *Clinical Neurophysiology*, *113*, 767-791.

Wolpaw, J. R., & Tennissen, A. M. (2001). Activity-dependent spinal cord plasticity in health and disease. *Annu. Rev. Neurosci*, *24*, 807-843.

Wolters, A., Sandbrink, F., Schlottmann, A., Kunesch, E., Stefan, K., Cohen, L. G., et al. (2003). Temporally asymmetric hebbian rule governing plasticity in the human motor cortex. *J Neurophysiol*, *89*, 2339–2345.

Woodin, M. A., Ganguly, K., & Poo, M. ming. (2003). Coincident pre- and postsynaptic activity modifies gabaergic synapses by postsynaptic changes in cl(-) transporter activity. *Neuron*, *39*, 807-820.

Yazawa, S., Shibasaki, H., Ikeda, A., Terada, K., Nagamine, T., & Honda, M. (1997). Cortical mechanism underlying externally cued gait initiation studied by contingent negative variation. *Electroencephalography and clinical Neurophysiology*, *105*, 390-399.

Ziemann, U., Iliac´, T. V., Pauli, C., Meintzschel, F., & Ruge, D. (2004). Learning modifies subsequent induction of long-term potentiation-like and long-term depression-like plasticity in human motor cortex. *The Journal of Neuroscience*, *24*, 1666-1672.

Ziemann, U., Paulus, W., Nitsche, M. A., Pascual-Leone, A., Byblow, W. D., Berardelli, A., et al. (2008). Consensus: Motor cortex plasticity protocols. *Brain Stimulation*, *1*, 164-182.

APPENDIX A

Plasticity

In this chapter the concept of neural plasticity is introduced and some of the likely mechanisms responsible for neural plasticity are discussed. Initially Hebbian plasticity is introduced followed by a review of synaptic plasticity. The next two sections introduce the concept of spike-timing dependent and homeostatic plasticity. The chapter ends with a description of cortical reorganization. The chapter was written by Mads Jochumsen as a part of the 9th semester [Jochumsen & Jensen, 2011]. The chapter is only used as a reference.

A functioning brain needs to be able to adapt and respond to new environments, learn and recover from temporary or sustained injury [Thickbroom, 2007]. The entity referred to as plasticity is a term that covers the mechanisms that the CNS depend on for adaptation. Some of these mechanisms will be reviewed in the following sections.

A.1 Hebbian plasticity

In the 1949 book *The Organization of Behavior: A Neuropsychological Theory* Donald Hebb postulated the following, which underlies some of the current thinking of plasticity:

- "*When an axon of cell A is near enough to excite cell B and repeatedly or persistently takes part in firing it, some growth process or metabolic change takes place in one or both cells such that A's efficiency, as one of the cells firing B, is increased.*"' [Hebb, 1949]

This postulate did not include mechanisms for decreasing the synaptic weights, but he eluded this in a previous postulate.

A.2 Synaptic plasticity

In neuroscience changes in synaptic efficacy between two neurons are believed to be a substrate for learning and memory [Buonomano & Merzenich, 1998]. Long-term potentiation (LTP) and long-term depression (LTD) are the most understood models of synaptic plasticity.

LTP results from coincident activity of pre- and post-synaptic neurons, which lead to a facilitation of chemical transmission between the two neurons, the effect can last for weeks or months [Abraham et al., 2002]. While LTP enhances the synaptic efficacy, LTD is the converse process that leads to a long lasting decrease in synaptic efficacy [Cooke & Bliss, 2006]. Some of the building blocks, which modulate LTP and LTD, in the glutamergic synapses, are the two receptors; N-methyl-D-aspartate (NMDA) and α-amino-3-hydroxy-5-methyl-4-isoxazolepropionic acid (AMPA), and the two types of ions; Ca^{++} and Mg^{++}. LTP and LTD are thought to reflect lasting changes, mediated by NMDA receptors, in the permeability or number of AMPA receptor channels. The activation of NMDA receptors depends on the activation of pre and post-synaptic neurons, which is in agreement with Hebb's postulate. The NMDA receptor activation is dependent on the Ca^{++} and Mg^{++} kinetics [Malenka & Bear, 2004][Thickbroom, 2007]. A model of the LTP/LTD is shown in figure A.1.

Glutamate, released pre-synaptically, binds to NMDA and AMPA receptors to open these channels. The influx of cations (Ca^{++}) is prevented by a voltage-gated magnesium block (Mg^{++}) in the NMDA receptor. The magnesium block is removed when there is a sufficient post-synaptic depolarization; this leads to an influx of Ca^{++}. When glutamate binds to AMPA receptors they become permeable to cations such as K^+ and Na^+, the influx generates an excitatory post-synaptic potential (EPSP) that serves as a basis for generation of action potentials. These mechanisms trigger synaptic plasticity. The effect of Ca^{++} influx is mediated by calmodulin (CaM). CaM triggers different signal pathways depending on Ca^{++} kinetics. CaM has two Ca^{++} binding sites, a carboxyl (C) site and an amino (N) lobe. When there is a rapid increase in Ca^{++} concentration C-lobe binding occurs, which increases the number and permeability of AMPA receptors. The increase in permeability outlasts the Ca^{++} influx. The increase in AMPA receptor number and permeability corresponds to LTP of the synapse. The same glutamate that has been released from the pre-synaptic neuron can now contribute to an even bigger EPSP. When there is a slower increase in the post-synaptic Ca^{++} concentration N-lobe binding occurs, which decreases the number and permeability of AMPA receptors. CaM and the kinetics of Ca^{++} reflect the balance between LTP and LTD (see [Bliss et al., 2003; Thickbroom, 2007] for a review of the above mentioned mechanisms). It should be noted that the molecular mechanisms described for induction and maintenance of LTP may vary from synapse to synapse [Cooke & Bliss, 2006].

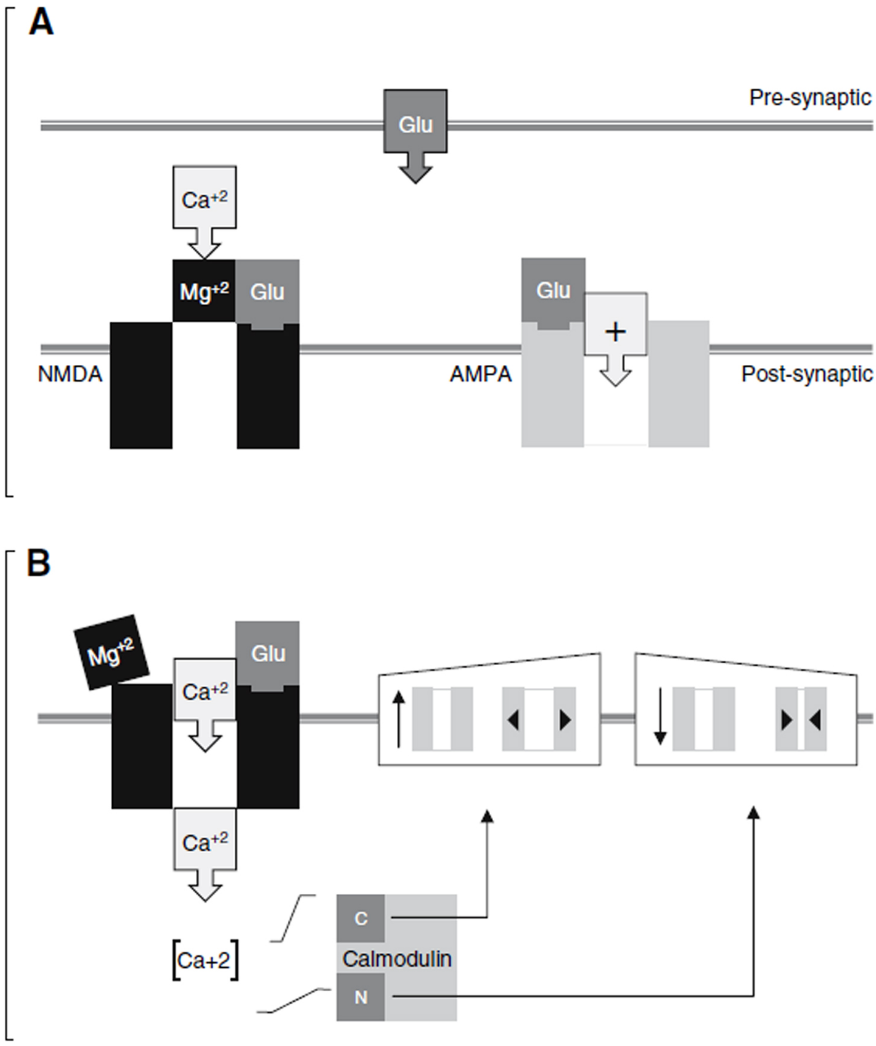

Figure A.1: *In the top of the figure (A) the effect of pre-synaptically released glutumate (Glu) on post-synaptic NMDA and AMPA receptors is shown. When glutamate binds to the AMPA receptors it becomes permeable to cations. The NMDA receptor needs to be activated when glutamate binds to the receptor to remove the Mg^{++} block. In the bottom of the figure (B) the effect of Ca^{++} and CaM is shown. When Ca^{++} binds to the C-lobe of CaM, the number and permeability of AMPA receptors increase. Ca^{++} that binds to the N-lobe will decrease the number and permeability of AMPA receptors. Page 585 in [Thickbroom, 2007].*

A.3 Spike-timing dependent plasticity

Synaptic strength can either be potentiated or depressed depending on the timing of spikes (action potentials). If the post-synaptic spike follows a pre-synaptic input within 10 ms there is a high potentiation. When the post-synaptic spike proceeds a pre-synaptic input the synaptic strength is depressed (see figure A.2) [Thickbroom, 2007]. Spike-timing dependent plasticity has also been observed in GABAergic (gamma-aminobutyric acid) inhibitory synapses. If post-synaptic spiking is properly timed with a glutamergic input, GABA inhibition will be reduced [Woodin et al., 2003].

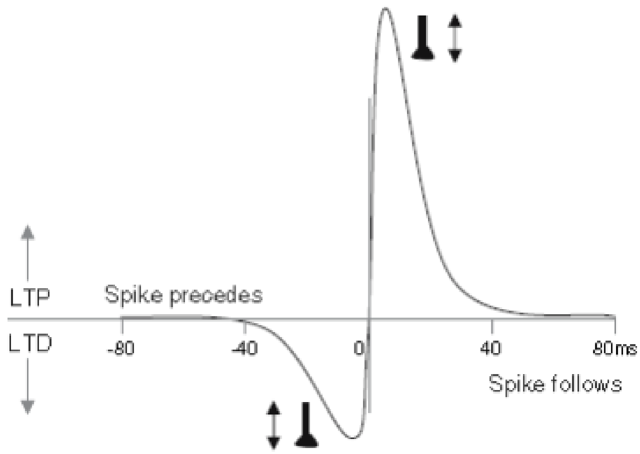

Figure A.2: *If the post-synaptic spike follows a pre-synaptic input within 10 ms there is a high potentiation. When the post-synaptic spike proceeds a pre-synaptic input the synaptic strength is depressed. Time 0 corresponds to the pre-synaptic input. Based on [Thickbroom, 2007] page 589.*

A.4 Homeostatic plasticity

Homeostatic plasticity can modulate the activity of synapses and thereby the excitability of neurons. In figure A.3 the effect of homeostatic plasticity following injury is shown [Rich & Wenner, 2006].

In the control, before injury, *Cell 1*, *Cell 2* and the cell inputs have normal levels of activity (yellow). When there is an injury some of the excitatory inputs to *Cell 1* are removed. The reduced activity could trigger different forms of synaptic compensation; two of them are shown in the figure. The first form of compensation is an increase of the strength to the remaining synaptic inputs to *Cell 1*, which may bring back the original level of excitability of *Cell 1*. The second form of compensation is an increased output from *Cell 1* to *Cell 2*, *Cell 1* will not recover the original level of excitability, but a change in activity may be induced in *Cell 2* and another part of the neuronal network.[Rich & Wenner, 2006]

A.5 Cortical representational plasticity

Somatotopic maps of the skin surface exist in the somatosensory cortex, which means that adjacent cortical regions correspond to adjacent skin sites [Merzenich & Sameshima, 1993]. These maps are not static, but changes in response to manipulation of peripheral input and behaviorally experience, the cortex is able to allocate areas in a use-dependent way. One possible mechanism responsible for

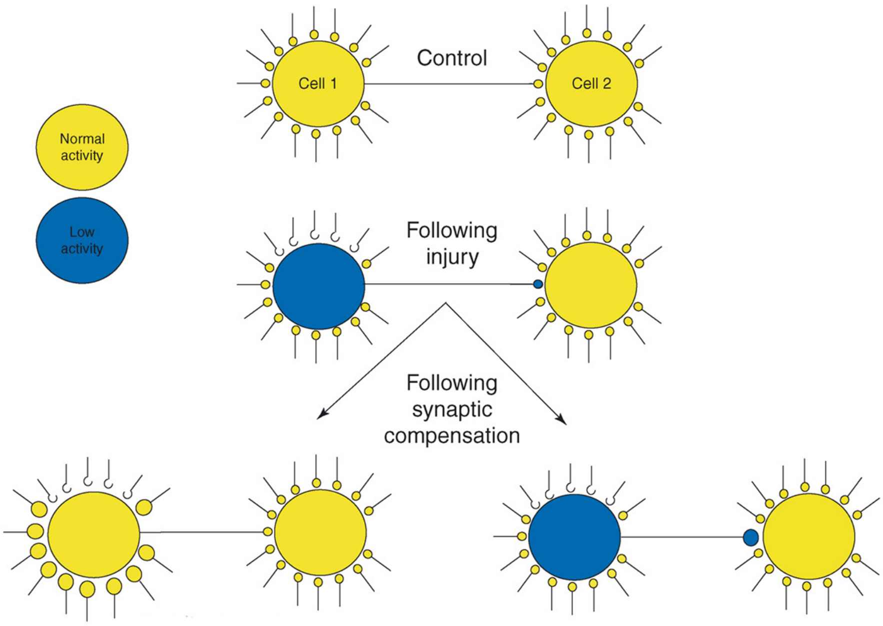

Figure A.3: *In the control, before injury, Cell 1, Cell 2 and the cell inputs have normal levels of activity (yellow). When there is an injury some of the excitatory inputs to Cell 1 are removed. Two compensation mechanisms are shown. The first form of compensation is an increase of the strength to the remaining synaptic inputs to Cell 1, which may bring back the original level of excitability of Cell 1. The second form of compensation is an increased output from Cell 1 to Cell 2, Cell 1 will not recover the original level of excitability, but a change in activity may be induced in Cell 2 and another part of the neuronal network. Page 120 in [Rich & Wenner, 2006].*

changes in the cortical representational plasticity is believed to be synaptic plasticity, mainly LTP following Hebb's postulate, however, the link between synaptic and cortical representational plasticity is not clear [Hebb, 1949][Buonomano & Merzenich, 1998]. A learning rule based on Hebb's postulate is to relate the detection of temporally correlated inputs. Looking at excitatory intracortical connections in cortical networks, neurons activated by behaviorally important stimuli respond to them in a more coherent temporal manner, according to the Hebbian learning rule. Detection of the temporally correlated inputs provide a mechanism for generating cortical cell assemblies that respond to specific stimuli and for the formation of topographic maps [Buonomano & Merzenich, 1998].
Cortical representational plasticity is affected by nerve transecting (e.g. median nerve transecting), but such a manipulation does not result in a permanent large area of the sensory cortex that is unresponsive; a reorganization of the somatotopic map takes place [Merzenich et al., 1983]. Immediately after the nerve transection, input from the adjacent skin areas is unmasked in the cortex representing the transected nerve. The unmasking is believed to be a result of existing

connections (thalamocortical input or horizontal connections) that have been suppressed by inhibitory circuits before the nerve transection [Merzenich et al., 1983][Buonomano & Merzenich, 1998]. Cortical representational plasticity may also be altered by skill-learning. If there is a relative increase in a specific subset of inputs, which does not suppress other inputs to other parts of the cortex, the representational area of the cortex to that subset of inputs can increase [Jenkins et al., 1990].

The plasticity of the motor cortex has been found to be modulated by motor performance and motor imagery [Abbruzzese et al., 1999][Fadiga et al., 1998][Pascual-Leone et al., 1995]. In motor learning tasks it has been found that the motor output area of a target muscle will increase [Pascual-Leone et al., 1995][Pearce et al., 2000]. An example of the increased motor output area of a target muscle is seen in Braille readers, their cortical representation of their reading finger was larger than the control group, which was blindsighted non-readers [Pascual-Leone et al., 1993]. It has also been reported that there is a decrease of intracortical inhibition [Pascual-Leone et al., 1995].

APPENDIX B

Discrete Wavelet Transform and Marginals

The DWT was used as a pre-processing technique, but it did not show any improvement of the classification accuracies. The DWT marginals were used as features for MRCP classification, but the classification accuracies were impeded when the DWT marginals were included in the feature vector. In this chapter the theory about the DWT and calculation of DWT marginals are summarized.

B.1 DWT

The DWT projects the signal into a set of basis functions that are delayed and scaled versions of a prototype function called '*mother wavelet*'. The success of using the DWT depends on the mother wavelet, which should reflect the morphology of the MRCP. To obtain the projection coefficients, multiresolution analysis (MRA) is used, it is implemented through the use of several digital filters (see figure B.1). The wavelet coefficients from the representation of the signal at several scales lead to frequency subbands with an equal width on a logarithmic scale. The digital filters, h and g, are used in the MRA to compute the DWT. The mother wavelet (ψ) and scaling function (θ) are related to h and g by equation B.1 and B.2, respectively. [Farina et al., 2007; Mallat, 1989; Polikar, 2006]

$$\psi(\frac{t}{2}) = \sqrt{2} \cdot \sum_{n} g[n] \cdot \theta(t-n) \tag{B.1}$$

$$\theta(\frac{t}{2}) = \sqrt{2} \cdot \sum_{n} h[n]\theta(t-n) \tag{B.2}$$

The approximation and detail coefficients of the DWT are calculated using equation B.3, and B.4 which is the inner product of the signal and the scaling function (approximation coefficients), and the inner product of the signal and the wavelet function (detail coefficients). In equation B.3 and B.4 j is the level of the DWT.[Polikar, 2006]

$$a(j,k) = \left\langle x(t), 2^{\frac{-j}{2}} \cdot \theta(2^{-j} \cdot t - k) \right\rangle \tag{B.3}$$

$$d(j,k) = \left\langle x(t), 2^{\frac{-j}{2}} \cdot \psi(2^{-j} \cdot t - k) \right\rangle \tag{B.4}$$

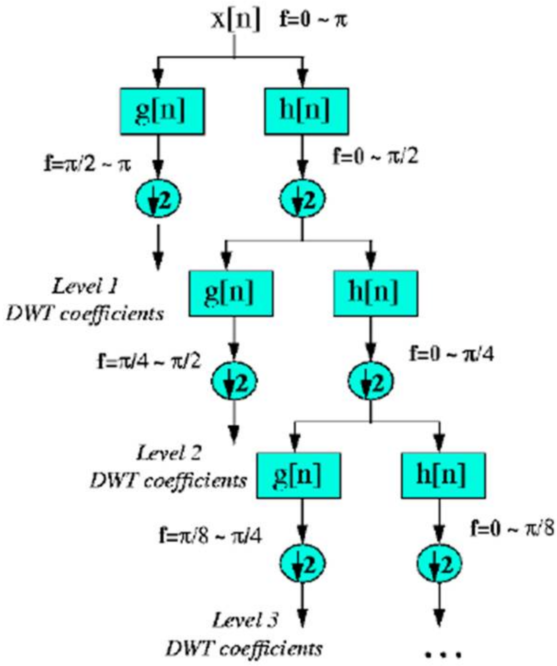

Figure B.1: *The subband coding algorithm. [Polikar, 2006]*

B.2 DWT Marginals

When a mother wavelet was selected (Daubechies 4) the DWT provides a set of approximation (equation B.3) and detail coefficients (equation B.4), which was found by the digital filters, h and g used for the MRA. The features (representing the signal x) used for classification were the components of the vector $M_x = [m_x(1), \ldots, m_x(\mathrm{J})]$. The vector contained information on how the wavelet coefficients were distributed over J bands. The vector represented the contribution of each frequency band (calculated from a dyadic scale) to the signal with a chosen analyzing mother wavelet. The feature vector was found from the following equations:

$$m_x(j) = \sum_{k=0}^{N/2^j-1} c_x(j,k),\; j = 1, \ldots, J \tag{B.5}$$

$$c_x(j,k) = \frac{|d_x(j,k)|}{\sum_{j=1}^{J} \sum_{k=0}^{N/2^j-1} |d_x(j,k)|} \tag{B.6}$$